GL02330

NASH

Toulmin, P., III, and Barton, P. B., Jr., 1964, A thermodynamic study of pyrite and pyrrhotite: Geochim. et Cosmochim. Acta, v. 28, p. 641–671.

Tuttle, O. F., and Gittins, J., 1966, Carbonatites: New York, Interscience, 591 p.

Tyler, R. C., and King, B. C., 1967, The pyroxenes of the alkaline igneous complexes of eastern Uganda: Mineralog. Mag., v. 36, p. 5–21.

Van Der Veen, A. H., 1963, A study of pyrochlore: Verh. Kon, Nederlands Geol. Minjbou. Gen., Geol. Ser. 22.

Van Wambeke, L., 1964, Geochimie minerale des carbonatites du Kaiserstuhl, in les roches

...—, Petrochemical studies on the alkalic rocks of Morotu district, Sakhalin: Geol. Soc. America Bull., v. 64, p. 769–810.

Riehle, J. R., McKee, E. H., and Speed, R. C., 1972, A Tertiary volcanic center, west-central Nevada: Geol. Soc. America Bull., v. 83, p. 1383-1396.

Manuscript Received by the Society July 12, 1971

Revised Manuscript Received November 1, 1971

PRINTED IN U.S.A.

JAMES R. RIEHLE *State University of New York at Binghamton, Binghamton, New York 13901*

EDWIN H. McKEE *U.S. Geological Survey, Menlo Park, California 94025*

ROBERT C. SPEED *Northwestern University, Evanston, Illinois 60201*

Tertiary Volcanic Center, West-Central Nevada

ABSTRACT

The Clan Alpine Mountains, Churchill County, Nevada, contain two sequences of Tertiary rhyolite tuffs and flows which are contemporaneous but markedly different in structure and thickness. The sequence in the northern part of the range consists of about 500 m of well-stratified ash-flow sheets of age range 22 to 30 m.y. The southern part of the range contains an assemblage of lava flows, domes, and ash-flow and epiclastic tuff beds, which is here subdivided into five mappable units. Radiometric ages are 22 to 30 m.y. Based on gravimetric analysis, the thickness of the southern sequence is at least 3,000 m and perhaps 5,000 m. The contact of the two rhyolite sequences, which is now largely eroded, was probably an abrupt gradation close to the present northern margin of the southern sequence.

Structural evidence indicates that the voluminous eruptions of the southern sequence were probably from local sources and were concurrent with faulting such that the rocks were deposited in one or more volcano-tectonic depressions. Recognition of the north wall of at least one caldera within the southern sequence seems clear. Age relations indicate that the vents for the southern sequence were probably the source of at least some of the ash flows of the northern sequence. Similar age and structural relations between different sequences of rhyolite tuffs and flows in the next range east, the Desatoya Mountains, suggest that the volcano-tectonic feature of which the southern sequence is a part extended east of the Clan Alpine Mountains.

INTRODUCTION

The Clan Alpine Mountains in west central Nevada contain two sequences of Tertiary rhyolite tuffs and flows which are contemporaneous but remarkably different in structure and thickness (Fig. 1). The southern half of the range (Figs. 2 and 3) is underlain by rhyolite that may be as much as 5,000 m thick and which occurs as lava flows, breccias, intrusive domes, and welded tuffs, which at most places are densely compacted. The age range of these rocks is 22 to 30 m.y.

The northern part of the range (Fig. 2) contains sheets of well stratified, variably compacted ash-flow tuff in sections up to 500 m thick. Most of these sheets can be traced to the east of the northern part of the Clan Alpine Mountains (McKee and Stewart, 1971); on the basis of reconnaisance mapping we consider that some of the sheets probably extend to the west and north as well. Ages of the ash-flow sheets in the northern Clan Alpine Mountains and of the correlative sheets in the northern New Pass Range are 23 to 30 m.y. These ash-flow sheets may have been derived in part from the southern Clan Alpine Mountains, the previously unrecognized volcanic center.

This paper focuses on the lithic properties of the southern sequence and its major structural features to explain the apparently large differences between the southern and the northern sequences. The northern sequence is a simple accumulation of widespread ash-flow sheets. The southern sequence appears to be derived from local sources in a volcano-tectonic depression, probably a series of calderas which were concurrent with volcanism. The similar durations of eruption of the northern and southern sequences support the proposition that the ash-flow sheets of the northern Clan Alpine Mountains and perhaps elsewhere had their source in the southern Clan Alpine Mountains. Lateral lithic changes in the ash-flow sheets, however, do not provide clear support for this hypothesis.

TERTIARY UNITS OF THE SOUTHERN CLAN ALPINE MOUNTAINS

The Tertiary rocks of the southern Clan Alpine Mountains are subdivided into eight mappable units. The distribution of these units is shown on Figure 3 and their sequence is shown on Figure 4. Each unit described is lithologically heterogeneous and consists of many rock types that have a spatial, temporal, and petrologic association. Six of the units are rhyolite in composition, and five of these constitute the main mass of a volcanic center which is the focus of this paper. Underlying the rhyolite units of the volcanic center is a unit composed of older andesitic rocks, and above them is a unit composed of younger rhyolite tuff beds and a unit composed of still younger basalt and andesite flows. A description of each unit follows.

Andesite Unit (Tha, Fig. 3)

The basal Tertiary unit in the Clan Alpine Mountains comprises hornblende and pyroxene andesite lava flows and epiclastic rocks composed mainly of andesite clasts. The unit lies unconformably on pre-Tertiary rocks and is overlain by rhyolite units. A K-Ar age on hornblende from a lava flow in the andesite unit is 35 m.y. (Table 1). Similar basal Tertiary andesite units are widespread to the east in Lander County (McKee and Silberman, 1970) and White Pine County (Blake and others, 1969), where their average age is also about 35 m.y.

The distribution and thickness of the andesite unit is highly irregular in the Clan Alpine Mountains. At places, the unit wedges out and younger rhyolite units lap over on pre-Tertiary rocks; elsewhere, the andesite unit is as thick as 800 m. The stratigraphic sequence of lava flows and intercalated epiclastic rocks varies laterally. At Byers Canyon, hornblende andesite lava flows lie below nonhornblendic lava flows, and still higher in the section, epiclastic rocks are dominant. Conversely, at Bernice Canyon, the lower 100 to 200 m of the section are chiefly epiclastic rocks and pyroxene andesite lava flows, and several hundred feet of hornblende andesite lava flows cap the section. The variability of thickness, stratigraphy, and the large quantity of intercalated epiclastic rocks indicates that the lava flows did not spread great lateral distances and that rapid

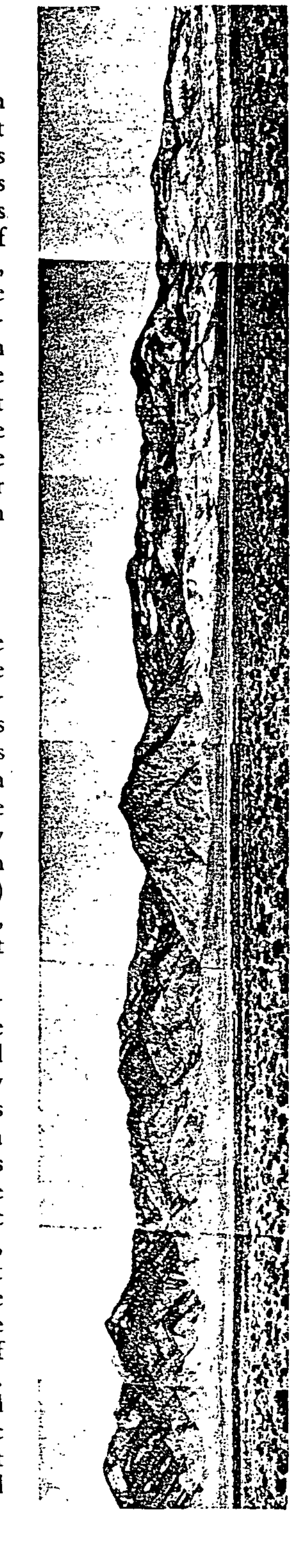

Figure 1. Photo of Clan Alpine Mountains looking west. The northern part of the range (right side of photo) is characterized by a sequence of well-stratified ash-flow sheets. The southern part is made up of a thick heterogeneous complex of lava flows, tuffs, and shallow intrusive rocks.

erosion and fluvial redistribution of materials occurred during the eruptive episode.

Andesite lava flows lie in places below rhyolite of both the ash-flow sheet sequence in the northern part of the Clan Alpine Mountains and the thick flow and intrusive complex of the southern part of the range. There seems to be no obvious relation between the occurrence or lithology of the andesite unit and the lithology of the succeeding rocks. Moreover, the wide distribution of andesite of similar age in central Nevada supports the assertion that eruption of the andesite unit in the southern Clan Alpine Mountains was probably unrelated to the later development of the rhyolite complex there.

Zoned plagioclase grains compose from 20 to 30 percent by volume of the andesite lava flows; An contents of individual grains range from An_{30} to An_{60}. High-calcium clinopyroxene ($2V_z = 50°$), which is usually altered, makes up from 5 to 15 percent of the rock, and hornblende composes from 0 to 25 percent. A single whole-rock analysis of a sample obtained from a hornblende-bearing andesite lava flow from Crescent Canyon is given in Table 2. This sample contains 17 percent plagioclase, 21 percent hornblende, and 6 percent pyroxene in a finely crystalline groundmass composed of plagioclase grains and undeterminable interstitial material. Its total iron content is less than 10 percent, it is quartz-normative, and plagioclase phenocrysts are strongly zoned with cores containing up to 60 percent An molecule. These features are characteristic of calc-alkaline andesite (Yoder, 1969).

Rhyolite Units of the Volcanic Center

Basal Composite Unit (Tr1, Fig. 3). The basal rhyolite unit of the southern Clan Alpine Mountains is an assemblage of ash-flow tuff beds, epiclastic tuff beds, and dense homogeneous rhyolite bodies. On the west flank of the range, the unit consists predominantly of ash-flow tuff beds greater than 300 m thick, locally interlayered with bedded tuff of probable lacustrine origin. On the east flank of the range, rhyolite flows of this unit consist predominantly of lenticular bodies of dense rhyolite, apparently restricted in areal extent. Such rhyolite bodies display no compaction zonations, suggesting that they are lava flows rather than welded ash flows. They contain, however, vague elliptical patches a few millimeters in length interpreted as pumice clasts, and they lack the conspicuous foliation which exists in massive rhyolite, more clearly interpreted as lava in younger units in the range. Thus, the mode of emplacement of the dense rhyolite bodies is uncertain. In sharp contact with the dense rhyolite bodies are lenticular bodies of noncompacted lithic tuff, locally well sorted and stratified. Such tuffs are probably of epiclastic derivation; in other lenticular bodies, however, local compaction variations suggest a pyroclastic origin. The basal composite unit is characterized by its lithologic heterogeneity which contrasts with the relatively uniform lithology of the rhyolite lavas of the overlying unit.

The base of the composite unit is unconformable with the andesite unit and pre-Tertiary rocks. Above the andesite, interbeds of sedimentary rocks composed largely of andesite clasts occur in the rhyolite sequence near its base. The thickness of the composite unit varies from 100 to greater than 600 m. In spite of the wide range of texture and type of eruption among the rocks assigned to the composite unit, they have a petrologic unity. The phenocryst population is characteristically moderately high, 15 to 30 percent of the first cycle deposits. Plagioclase is relatively abundant; oligoclase/sanidine varies from 1/1 to 3/1. Quartz seldom exceeds 5 percent. Chemical analyses of six relatively nonporous specimens from the basal unit are in Table 2. The normative feldspar composition of these rocks indicates that they are rhyolite (Fig. 5) according to the classification of O'Connor (1965).

The age of the composite unit in the central Clan Alpine Mountains has not been obtained radiometrically, but we believe this unit is conformable with the overlying unit dated at 30 m.y.

Uniform Dense Rhyolite (Tr2, Fig. 3). The second rhyolite unit consists predominantly of dense, foliated rhyolite flows with only local tuff intercalations between 15 and 100 m thick. It is distinguished from the basal composite unit by its comparatively uniform, dense, well-foliated rocks; in contrast, the composite unit contains a large amount of noncompacted pyroclastic rocks. Though the uniform dense rhyolite unit is apparently laterally continuous over much of the map area (Fig. 3), the thickness varies markedly, from zero to a maximum of 200 m at War Canyon. The contact between the composite unit and

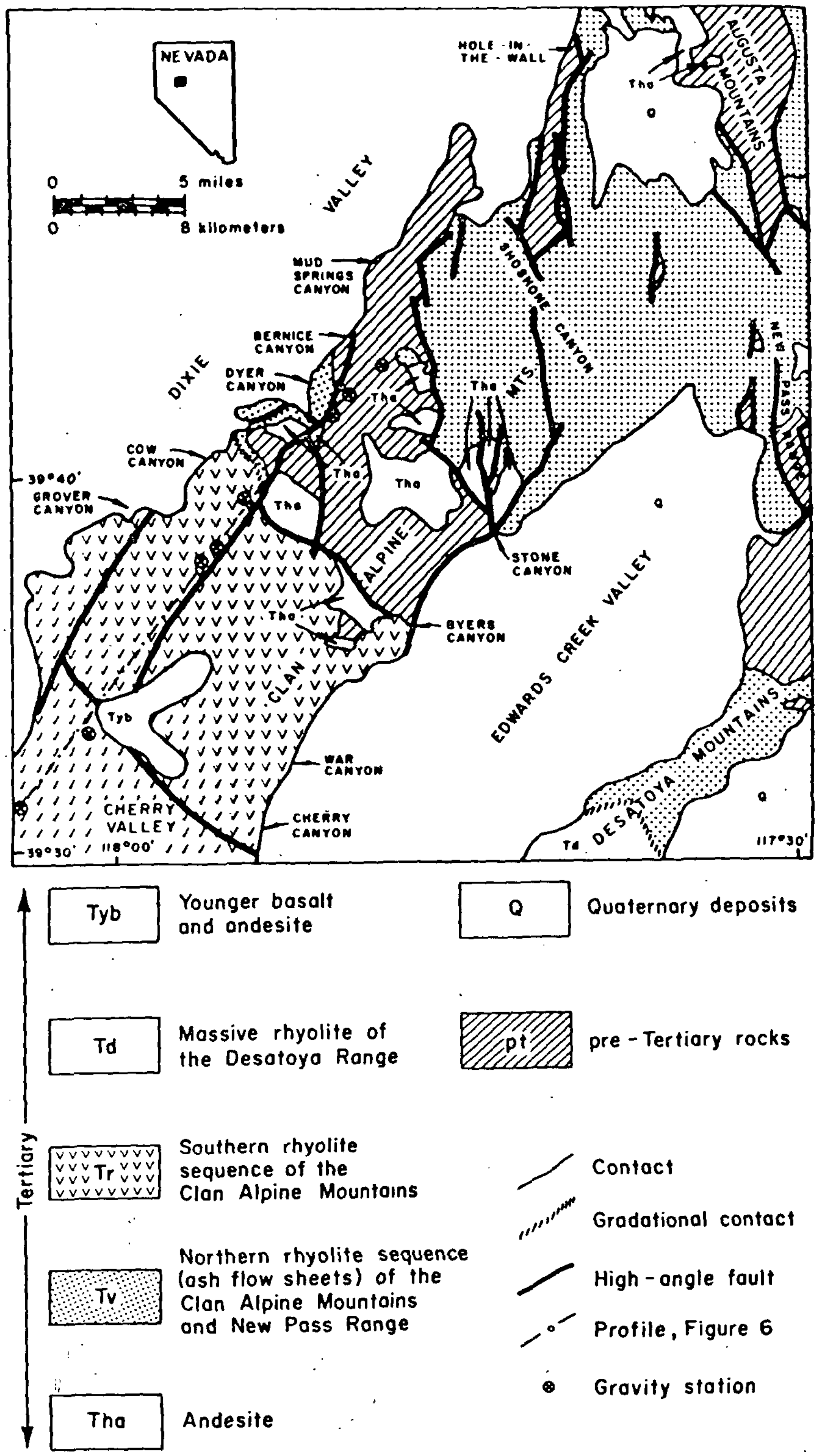
NEVADA
0 5 miles
0 8 kilometers
VALLEY
HOLE-IN-THE-WALL
AUGUSTA MOUNTAINS
Tha
Q
MUD SPRINGS CANYON
SHOSHONE CANYON
BERNICE CANYON
DIXIE
DYER CANYON
MTS.
NEW PASS RANGE
COW CANYON
39°40'
GROVER CANYON
ALPINE
STONE CANYON
EDWARDS CREEK VALLEY
BYERS CANYON
CLAN
Tyb
WAR CANYON
CHERRY VALLEY
CHERRY CANYON
DESATOYA MOUNTAINS
Td
39°30'
118°00'
117°30'
Tertiary
Tyb Younger basalt and andesite
Td Massive rhyolite of the Desatoya Range
Tr Southern rhyolite sequence of the Clan Alpine Mountains
Tv Northern rhyolite sequence (ash flow sheets) of the Clan Alpine Mountains and New Pass Range
Tha Andesite
Q Quaternary deposits
pt pre-Tertiary rocks
Contact
Gradational contact
High-angle fault
Profile, Figure 6
Gravity station

the uniform dense rhyolite unit is conformable, and there is no evidence for an erosional hiatus between the two units.

Foliation in the dense rhyolite unit is a millimeter-scale lamination caused largely by grain size changes in devitrification products; the individual laminae are generally continuous over several centimeters. The foliation attitude is highly variable in relation to the configuration of unit boundaries; changes of foliation attitude occur over several tens to hundreds of meters. Foliations of rocks in the dense rhyolite unit are distinguished from those of the overlying unit, in which the foliations are continuous over several meters and variations of attitude may occur over a few centimeters. There is little evidence that the foliation of the dense rhyolite unit was originally a compaction fabric, and we interpret the foliation as resulting from shear during flow of rhyolite lavas.

Phenocryst contents of individual flows in the dense rhyolite unit vary widely; some flows contain less than 5 percent phenocrysts, whereas others contain up to 30 percent of quartz, oligoclase, and sanidine phenocrysts. A K-Ar age on sanidine from the dense rhyolite unit (Table 1) is 29.9 m.y. Two analyzed specimens of the unit are both classified as rhyolite (Table 2, Fig. 5).

Foliated Rhyolite (Trd, Fig. 3). Remarkably distinctive rhyolite occurs in intrusive domes between Grover and Cow Canyons on the west side of the range. The most obvious characteristic of this rhyolite is the pronounced millimeter-scale foliation which is generally steeply inclined and is locally highly folded on wavelengths of 1 cm to tens of meters; axes of the small folds impart a conspicuous rectilinear lineation to the rock. The deformation of the foliation occurred during flow because the subjacent unit is undeformed.

The stratigraphic relation of the foliated rhyolite unit to the dense rhyolite unit is not clear. Differences in the style of deformation of the foliation in the rhyolite of the two units have been previously described. In addition, the rhyolites differ by their phenocryst contents; the foliated rhyolite unit rarely has more than 5 percent phenocrysts, predominantly sanidine, whereas the dense rhyolite unit varies from crystal-poor to crystal-rich with much quartz in addition to sanidine and plagioclase. A fission-track age of an intrusive dome of foliated rhyolite is 29.9 ± 1.0 m.y. (Table 1). Considering the analytical precision of the age determinations, the dense rhyolite unit and the foliated rhyolite unit are contemporaneous.

The foliated rhyolite is completely devitrified, and the foliation consists of alternating devitrification textures. Coarser laminae are microcrystalline quartz and feldspar in series of clusters of radiating fibers. Quartz of possible secondary (hydrothermal) origin occurs in irregular patches up to 2 cm in diameter.

Outcrop patterns of individual domes are equidimensional and are 100 to 500 m in diameter. Portions of the domes consist of breccia of foliated rhyolite; foliation in the breccia clasts is randomly oriented in a matrix of massive rhyolite. Vertical to subvertical columnar joints cut the flow fabric of this unit.

Chemical analysis of a specimen of foliated rhyolite (Table 2) indicates the rock is subalkaline rhyolite, typical of Tertiary silicic rocks of the Basin and Range province.

Dark, Massive Rhyolites (Trf, Fig. 3). The dark, massive rhyolite unit occurs along the west flank of the range, in the vicinity of Grover Canyon (Fig. 3); the exact stratigraphic position of this unit is uncertain. Chemically, a sample of the unit is classified as rhyolite (Table 2, Fig. 5). Petrographically, the rocks of the unit most resemble dense, vaguely foliated rhyolite of the basal composite unit exposed on the east side of the range, because the total phenocryst content ranges from 10 to 25 percent, and there is a uniformly high degree of compaction. Phenocrysts are predominantly plagioclase with lesser amounts of quartz and sanidine. Conspicuous foliations are absent and the origin of the massive rhyolite unit as lava flows or pyroclastic deposits is uncertain. South of Grover Canyon the massive rhyolite unit is intruded by small domes of the foliated rhyolite unit, thereby placing a minimum limit on the possible age of the massive rhyolite unit at about 29 m.y. (Table 1, Trd 29.9 ± 1.0 m.y.). At the present we can suggest only that the massive rhyolite unit may comprise lavas associated with, and slightly older than, the intrusive domes of the foliated

Figure 2. Generalized geologic map of Clan Alpine Mountains showing distribution of southern and northern rhyolite sequences.

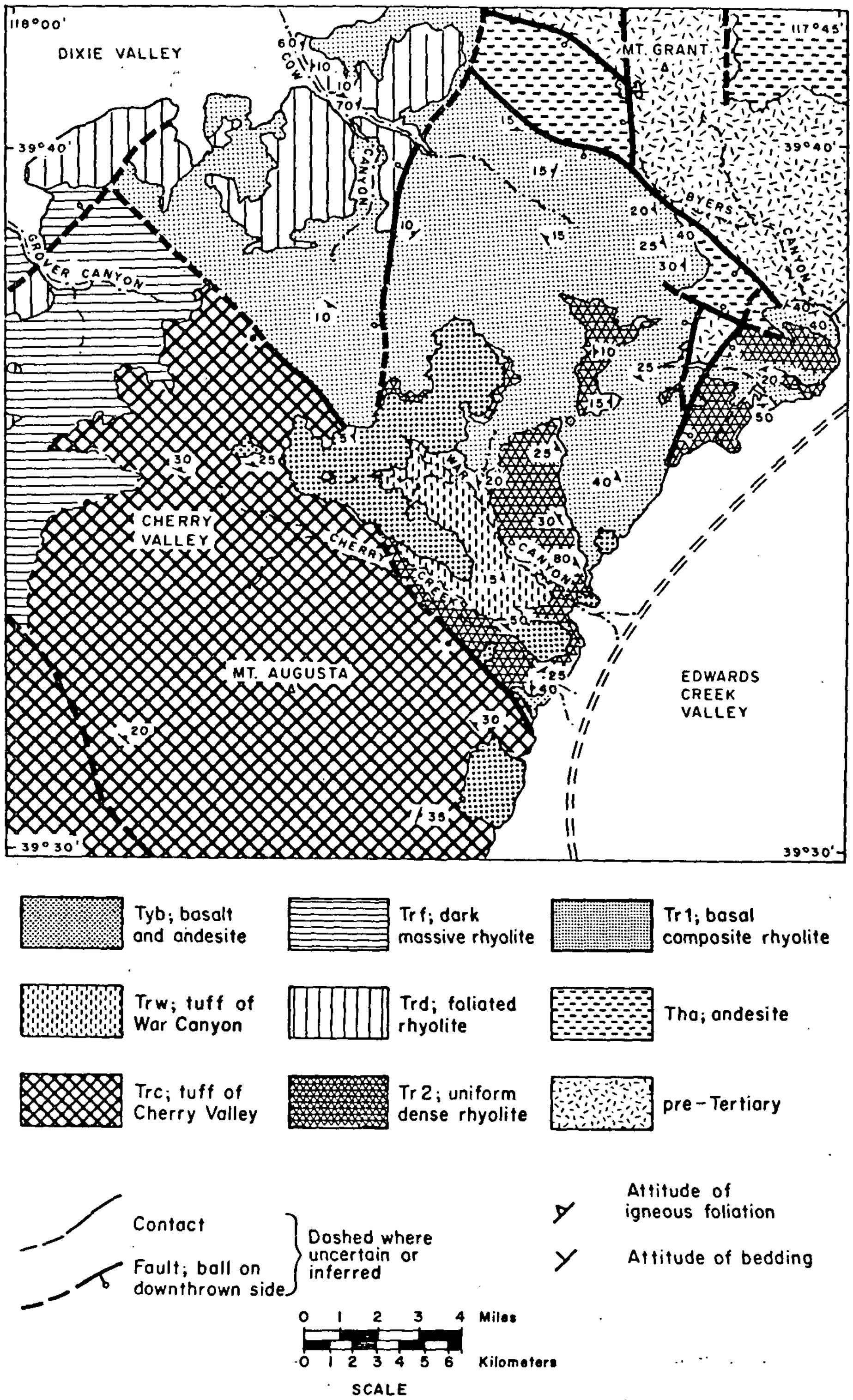

118°00'
117°45'
39°40'
39°30'
DIXIE VALLEY
MT. GRANT
BYERS CANYON
GROVER CANYON
COW CANYON
CHERRY VALLEY
CHERRY CREEK
WAR CANYON
MT. AUGUSTA
EDWARDS CREEK VALLEY
Tyb; basalt and andesite
Trf; dark massive rhyolite
Tr1; basal composite rhyolite
Trw; tuff of War Canyon
Trd; foliated rhyolite
Tha; andesite
Trc; tuff of Cherry Valley
Tr2; uniform dense rhyolite
pre-Tertiary
Contact
Fault; ball on downthrown side
Dashed where uncertain or inferred
Attitude of igneous foliation
Attitude of bedding
0 1 2 3 4 Miles
0 1 2 3 4 5 6 Kilometers
SCALE

rhyolite unit, or that the massive rhyolite unit may correlate with the composite rhyolite unit.

Crystal Tuff of Cherry Valley (Trc, Fig. 3). The southern half of the map area (Figs. 2, 3) is underlain by a unit of thick, uniform, densely compacted crystal tuff. The exposed thickness is about 1,500 m, but the base and top of the unit are missing. Within the map area the unit lies above only the rhyolites of the massive rhyolite unit; the unit of crystal tuff contacts all other units along a steep fault which strikes across the range. A K-Ar age on biotite from a sample of the unit of crystal tuff is 24.5 ± 0.8 m.y. (Table 1) indicating a distinctly younger age than for other units. The fault occurred after deposition of the uniform dense rhyolite unit (about 29 m.y.) and before a younger basalt flow (presumed to be less than 20 m.y. old) that overlaps the fault. Considering the thickness of the unit of crystal tuff unit its apparent restriction to the area south of the fault suggests that its distribution may be due to deposition in a fault-bounded basin.

On the east side of the range, the crystal tuff displays abundant eutaxitic textures, but other than a few vitrophyre lenses, compaction zonation is absent. Thus, to a first approximation, the unit here is a simple cooling unit 1,500 m thick. On the west flank of the range, however, boundaries between sucessive ash flows are recognized. There, the lower part of the section is generally a more poorly compacted lithic tuff, and the upper part is a more densely compacted eutaxitic crystal tuff. The stratigraphic equivalence of the lower parts of the unit of crystal tuff on the west and east sides of the range is uncertain.

Petrographically, the unit of crystal tuff is distinctive because of its uniformly high phenocryst content (20 to 30 percent) and its relatively high biotite abundance (3 to 5 percent). Zoned plagioclase (oligoclase-andesine) and sanidine phenocrysts together constitute about 15 to 30 percent of the rock; quartz phenocrysts are generally less than 5 percent. The matrix consists of collapsed and devitrified shards and pumice. Chemical analysis of a sample of the crystal tuff unit (Table 2) indicates that the rock is rhyolite, but the SiO_2 content is lower and CaO content is higher than other rhyolite units in the map area.

Rhyolite of War Canyon (Trw, Fig. 3)

A small unit of rhyolite crystal tuff occurs near the head of War Canyon. The tuff is a tabular body about 300 m thick which is unconformable on older rhyolite of the uniform dense rhyolite unit. The rhyolite of War Canyon contains compaction zonations which indicate the rock unit consists of two and perhaps three ash-flow cooling units. A K-Ar age of sanidine from this unit is 22.1 ± 0.7 m.y. (Table 1). The unit is the youngest silicic rock in the southern Clan Alpine Mountains.

Phenocrysts consist of quartz, 10 percent; plagioclase, 5 percent (andesine); and sparse biotite. Distinctive fiamme (ellipsoidal weathering features), most likely devitrified pumice, occur near the base of the unit. Analysis 11, Table 2, shows that the composition of a sample of the rhyolite of War Canyon is similar to the compositions of older rhyolites.

Younger Basalt and Andesite (Tyb, Fig. 3)

Basalt flows which cap the range crest (Fig. 3) and small andesite flows on the east face of the range are the youngest volcanic units in the Clan Alpine Mountains. These flows are equivalent to the relatively young mafic lavas which constitute the uppermost beds in many Tertiary sections of the Basin and Range province. We have not dated rocks of this unit

Figure 3. Geologic map showing distribution of Tertiary units, southern Clan Alpine Mountains. See text for description of units.

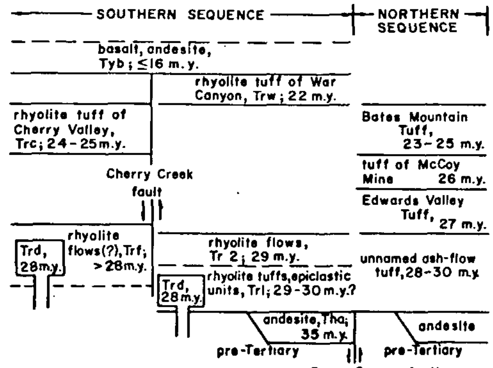

Figure 4. Schematic stratigraphic relations of the northern and southern sequences, Clan Alpine Mountains. Dashed lines indicate uncertain maximum or minimum ages.

TABLE 1. AGE DETERMINATIONS OF SPECIMENS FROM THE SOUTHERN SEQUENCE, CLAN ALPINE MOUNTAINS

Rock type and designation (Figure 3)	Location of sample	Mineral dated	K_2O percent	Ar^{40} rad $\times 10^{-11}$ m/g	percent Ar^{40} rad	Age, m.y.
Rhyolite crystal tuff (Trw)	117° 51' 40" 39° 35' 05"	Sanidine	10.42	34.17	58.5	22.1 ± 0.7
Rhyolite tuff, near Dyer Canyon*	117° 49' 20" 39° 43' 40"	Biotite	8.28	35.06	54.4	28.4 ± 1.0
Rhyolite dome (Trd)*	117° 53' 35" 39° 40' 30"	Zircon	fission track determination (5 grains)			29.9 ± 1.0
Rhyolite flow (Tr2)*	117° 49' 30" 39° 37' 15"	Sanidine	8.36	37.17	71.2	29.9 ± 1.0
Andesite flow, basal Tertiary unit (Tha)	117° 47' 50" 39° 38' 40"	Hornblende	0.965	5.00	57.3	35.0 ± 1.2
Rhyolite crystal tuff (Trc)	117° 54' 40" 39° 35' 15"	Biotite	8.36	30.46	47.1	24.5 ± 0.8
Basal ash flow tuff	117° 45' 30" 39° 48' 44"	Biotite	6.69	29.82	65.2	29.9 ± 1.0

*Rocks from the central Clan Alpine volcanic complex

Constants used in all K-Ar determinations are: $\lambda_\epsilon = 0.585 \times 10^{-10}\ yr^{-1}$

$\lambda_\beta = 4.72 \times 10^{-10}\ yr^{-1}$

$K^{40} / K_{total} = 1.19 \times 10^{-4}$ mole/mole

Fission track determination: ρ_s - spontaneous track density, average of 5 grains = 7.2×10^6 tracks/cm^2

$1/2\ \rho_i$ - induced track density, average of 5 grains = 9.3×10^6 tracks/cm^2

ϕ = neutron dose = 1.28×10^{15}

Decay constant used is $6.85 \times 10^{-17}\ yr^{-1}$

in the study area; eruption of basaltic lavas occurred as recently as the Pleistocene in the Carson Sink region to the west (Willden and Speed, unpub. data) whereas rocks of equivalent stratigraphic position to the east in Lander County are dated 10 to 16 m.y. (McKee and Silberman, 1970). Thus, 16 m.y. represents a possible maximum age for young lavas in the Clan Alpine Mountains.

Summary and Interpretation

The southern Clan Alpine Mountains contain an enormous volume of Oligocene and Miocene rhyolite which erupted in the interval 22 to 30 m.y. ago (Table 1). The rhyolite comprises two main eruptive phases, 28 to 30 m.y. and 24 to 25 m.y. Gravity models of the subsurface indicate that the earlier phase produced much more than the 240 cu km of rhyolitic lava and tuff now contained in the range (Fig. 6). The major characteristics of the earlier rhyolites are their obscure stratification and irregular lithosomal configuration. The older rhyolites consist of many small lava flows, ash flows, shallow intrusive domes, and volcanic sedimentary rocks. The occurrence of rhyolite domes demonstrates that local sources existed through at least part of the earlier eruptive phase. The local, lenticular, bedded,

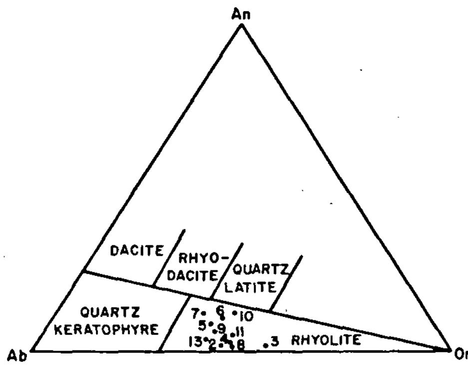

Figure 5. Rocks from southern sequence, Clan Alpine Mountains, classified according to O'Connor (1965). Numbers refer to analyses given in Table 1.

TABLE 2. WHOLE-ROCK ANALYSES AND WEIGHT PERCENT NORMS OF SPECIMENS FROM SOUTHERN CLAN ALPINE MOUNTAINS, NEVADA

Map unit	(1) Tha	(2) Trl	(3) Trl	(4) Trl	(5) Trl	(6) Tr2	(7) Tr2	(8) Trd	(9) Trf	(10) Trc	(11) Trw	(12) Tyb	(13) Intrusive dome, Cherry Creek fault (R-707)
Lab no.	M111655W	R-703	R-704	R-706	R-708	M111656W	R-705	M111657W	R-701	M111658W	M111659W	R-702	
Field no.	14667-1*	70-21†	69-2†	69-44†	68-90†	14667-2*	69-43†	14667-3*	70-15†	14667-4*	14667-5*	70-18†	68-66†
SiO_2	57.8	73.8	74.7	77.1	71.4	71.8	68.9	76.7	70.4	68.9	69.6	55.2	69.7
Al_2O_3	16.5	14.7	13.3	12.9	15.0	15.0	15.9	12.4	14.9	15.8	14.6	19.5	15.1
Fe_2O_3	5.0	1.6	1.9	.6	1.7	1.4	2.1	1.1	2.6	2.0	1.5	7.4	1.7
FeO	1.80	.12	--	.12	.60	.22	.52	.06	--	.50	.66	.68	.80
MgO	3.60	.18	.10	.10	.47	.27	.84	.06	.27	.45	.40	2.33	.25
CaO	5.3	.2	.5	.4	1.4	1.6	2.1	.3	1.0	1.8	1.8	7.1	.8
Na_2O	2.9	3.9	2.8	3.6	3.9	3.9	4.1	3.7	4.3	3.5	3.7	4.0	4.7
K_2O	2.8	4.8	5.5	4.7	4.1	4.4	4.0	4.8	4.8	4.6	4.8	2.2	5.0
H_2O+	1.80	1.02	.44	.65	.52	.39	.87	.29	.54	.80	.71	.50	.43
H_2O-	1.10	n.d.	n.d.	n.d.	n.d.	.57	n.d.	.21	n.d.	n.d.	.49	n.d.	n.d.
TiO_2	.99	.14	.12	.04	.26	.28	.34	.21	.53	.40	.29	1.17	.56
P_2O_5	.37	.06	.11	.03	.10	.04	.16	--	.14	.08	.02	.53	.15
MnO	.04	.04	.03	.02	.05	--	.08	--	.03	--	.04	.10	.05
CO_2	.05	<.05	<.05	<.05	.36	<.05	.20	<.05	.05	<.05	.85	.05	<.05
Total	100.	101.	100.	100.	100.	100.	100.	100.	100.	99.	99.	101.	99.
Weight norm													
q	15.0	32.3	36.6	37.9	29.7	29.3	25.1	36.6	24.5	27.1	25.8	7.0	21.6
or	17.0	29.0	32.7	27.8	24.6	26.0	23.8	28.4	28.9	27.8	29.0	12.9	29.6
ab	25.3	33.3	24.0	30.3	33.3	33.0	34.8	31.3	37.0	30.5	31.2	34.1	40.3
an	24.5	.8	1.5	1.9	6.5	7.7	9.3	1.5	4.3	8.4	8.8	29.0	2.8
c	--	2.81	2.2	1.3	1.8	1.2	1.5	.7	.9	2.0	.1	--	.9
en	9.2	.4	.3	.2	1.2	.7	2.1	.2	.7	1.2	1.0	5.1	.6
hm	3.0	1.6	1.9	.4	.8	1.4	1.5	1.1	2.6	1.7	.5	7.5	1.0
ap	.9	.1	.3	.1	.2	.1	.4	--	.3	.2	.1	1.2	.4
il	1.9	.3	.1	.1	.5	.5	.7	.1	.1	.8	.6	1.7	1.1
ru	--	--	.1	--	--	--	--	.1	.5	--	--	--	--
di	.1	--	--	--	--	--	--	--	--	--	--	1.6	--
tn	--	--	--	--	--	--	--	--	--	--	--	.8	--
mt	3.1	.1	--	.3	1.3	--	1.0	--	--	.5	1.4	--	1.1
Total	100.	101.	100.	100.	100.	100.	100.	100.	100.	100.	99.	101.	99.

*Analyses performed in Rapid Rock Analysis Lab. under L. Shapiro, U.S.G.S., Menlo Park, California.

†Analyst: Max Budd, S.U.N.Y. (Binghamton); methods of Shapiro and others (water-free basis).

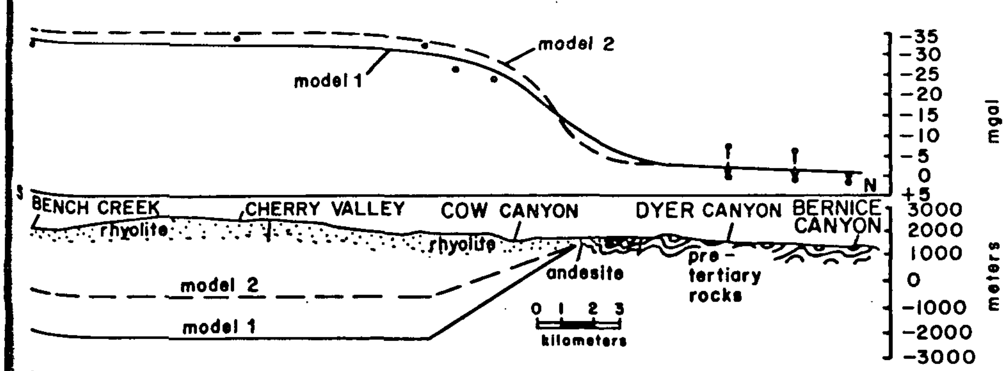

Figure 6. Geologic and gravity profile AA′, Figure 2. Open circles: simple Bouguer gravity values; closed circles: gravity values corrected for effect of Dixie Valley. Gravity models are two-dimensional configurations of the base of the southern rhyolite sequence relative to a substrate of postulated pre-Tertiary rocks and Tertiary andesite. Model 1: density contrast = 0.2 g/cc, solid line. Model 2: density contrast = 0.4 g/cc, dashed line.

tuffaceous rocks indicate the presence of small water-filled basins during the earlier eruptive phase. We envision that these characteristics were most likely produced in a volcanic center in which the topography was irregular and in which local viscous flows (lava and breccia) and more ubiquitous tuff could collect.

The later major eruptive phase of the southern Clan Alpine Mountains (24 to 25 m.y.) produced a single rhyolite unit remarkable for its uniformity throughout great thicknesses although its fabric seems one of a compacted tuff. In theory, successive ash flows should contain a discrete compaction reversal at each boundary unless the time duration between flows was very short, or succeeding flows were anomalously thick (Riehle, 1970). On the basis of this, we interpret the crystal tuff of Cherry Valley as resulting from rapid outpouring of large quantities of ash such that the compaction was effectively that of a single ash flow. Clearly, a depression—probably a caldera—allowed over 1,500 m of densely compacted tuff to accumulate in a brief period of time. The northern boundary of the unit of crystal tuff is a fault cutting older rhyolite, and it seems likely that this fault is the northern boundary of a caldera which was rapidly filled by the ash flows that produced the crystal tuff of Cherry Valley. The southern boundary of this caldera has not been mapped, but the continuity of the crystal tuff to the south in the Clan Alpine Mountains indicates the depression had a north-south dimension exceeding 19 km.

The preserved volume of the younger (22 m.y.) rhyolite of War Canyon is too small to indicate a major eruptive episode in the southern part of the Clan Alpine Mountains at that time. Moreover, this unit is an ash-flow sheet that may be widespread. Mafic lavas were extruded both earlier (35 m.y.) and later (16 m.y.) than the rhyolite complex, and owing to the widespread regional distribution of such lavas, there appears to be no relation between their eruption and the eruption of the rhyolite sequence of the southern Clan Alpine Mountains.

TERTIARY UNITS OF THE NORTHERN CLAN ALPINE MOUNTAINS

The general sequence of Tertiary rocks in the northern Clan Alpine Mountains is broadly similar chemically to that in the southern part of the range; that is, andesite-rhyolite-basalt or andesite.

The rhyolite sequence of the northern Clan Alpine Mountains differs markedly from that of the southern region. The northern sequence consists entirely of well stratified ash-flow tuff sheets in sections as much as 500 m thick. At Shoshone Creek (Fig. 2), the section is composed of at least 10 cooling units, most of which are correlative with units about 12 km southeast in the northern New Pass Range (McKee and Stewart, 1971). A tuff unit which is widespread at or near the base of the Shoshone Creek section is correlated with the 26 to 28 m.y. Edwards Creek Tuff of the New Pass Range. At most places north of Shoshone Creek in the Clan Alpine and Augusta Mountains, the Edwards Creek Tuff is at the base of the rhyolite sequences, but at Shoshone Creek, thin lenticular bodies of older tuff beds are locally below the Edwards Creek Tuff. Correlatives of the lenticular older tuff beds in the New Pass section may have K-Ar ages of 28.5 ± 1.0 and 30.3 ± 1.0 m.y. (McKee and Stewart, 1971). Upper units in the Shoshone Creek section have not been dated radiometrically, but they are believed to be correlative in part with the 23 to 24 m.y. Bates Mountain Tuff and overlying 22 m.y. tuff unit in the New Pass Range.

The northern rhyolite sequence is continuous for 10 to 12 km south from Shoshone Creek to Stone Canyon on the east flank of the Clan Alpine Mountains and Bernice Canyon on the west flank, where the rhyolite sequence is faulted against older rocks (Fig. 2). The thickness of the section of the ash-flow tuff sheets is about constant throughout the northern Clan Alpine Mountains, and the only marked change is the southward thickening of the pre-Edwards Creek tuff beds to about 100 m at the southernmost exposures. Here, the basal tuff unit is largely poorly compacted, but it contains several zones of moderate compaction which indicate the unit comprises multiple ash flows. A K-Ar age of biotite from the basal tuff unit which is in depositional contact with pre-Tertiary rocks 3 km north of Bernice Canyon is 29.9 ± 1.0 m.y. (basal ash-flow tuff, Table 1). This age provides support for the equivalence of the sections of ash-flow tuff sheets in the northern Clan Alpine Mountains and northern New Pass Range. The contact between the basal unit and the overlying Edwards Creek Tuff is everywhere conformable, which suggests that the basal unit was not widely eroded before emplacement of younger tuff units. Thus, the patchy distribution of the basal tuff unit near Shoshone Creek is probably due to infilling of irregular topography at the distal end of an ash flow.

Rhyolite is absent over a 6 km interval of the Clan Alpine Mountains between the northern and southern rhyolite sequences, except along the western margin of the range near Dyer Canyon (Fig. 2). Here thin erosion remnants of variably compacted ash-flow tuff beds lie unconformably on the 35 m.y. andesite unit and on pre-Tertiary rocks. Though the thickness of the remaining section is small, the rhyolite rocks at the mouth of Dyer Canyon and for 3 km south are structurally similar to rocks of the northern sequence but structurally different from most units in the southern sequence. About 3 km south of Dyer Canyon, the variably compacted tuff beds grade within a distance of a few hundred meters to a massive crystal lithic tuff bed assigned to the basal composite unit of the southern sequence (Figs. 2 and 3). Here the basal composite is overlain by the northernmost outcrops of foliated rhyolite which occur on the north flank of a large bulbous dome. If the ash-flow tuff beds near Dyer Canyon are correctly correlated with the northern sequence, the gradational contact between the ash-flow beds and the massive tuff bed south of Dyer Canyon represents the transition of this rhyolite unit from the southern to the northern sequence. Elsewhere in the range, the contact has been eroded, but evidence suggests that most other rhyolite units of the volcanic center in the southern part of the range did not spread much beyond their present location. They cannot be correlated with ash-flow tuff sheets of the northern sequence. Moreover, thickness of units and regional distribution suggests that the ash-flow tuff sheets of the northern sequence originally were continuous in the Clan Alpine Mountains only about as far south as the existing northern boundary of the southern sequence. This distribution of the two rhyolite sequences is also reflected by the exposure pattern of pre-Tertiary basement rocks. Exposure of the pre-Tertiary substrata occurs only beneath the northern ash-flow sheet sequence. The lack of a pre-Tertiary basement beneath the southern rhyolites indicates a precipitous thickening of rhyolitic rocks at the northern margin of the southern sequence.

The K-Ar ages of units in the southern sequence and the single ash-flow tuff bed that extends from the northern into the southern sequence overlap within analytical uncertainty, and suggest relatively rapid emplacement of most of the older rhyolite units of the southern sequence concomitantly as the basal unit of the northern sequence about 29 m.y. ago.

STRUCTURE OF THE TERTIARY UNITS

Figure 2 shows the distribution of exposed pre-Tertiary rocks in the Clan Alpine Mountains; the youngest layered rocks in this group are Middle Jurassic (Speed and Jones, 1969) indicating a significant hiatus between the pre-Tertiary and Tertiary rocks. There is a clear relation between widespread exposure of pre-Tertiary rocks and the occurrence of Tertiary ash-flow sheets of the northern rhyolite sequence. In the region of the southern rhyolite sequence, exposures of pre-Tertiary rocks are sparse. Because the oldest rhyolite units of both sequences are contemporaneous, the base of the southern sequence must be downset substantially below the base of the northern sequence. The minimum relative displacement is about 1,200 m as indicated by the elevation difference of the pre-Tertiary rocks on the range crest at Byers Canyon and the lowest level of the southern rhyolite sequence on the range flanks.

The southern edge of widespread outcrops of pre-Tertiary rock (Fig. 2) is in part a northwest-striking fault which brings the southern rhyolite sequence and the andesite unit against the older rocks. As presented earlier, the fault trace is believed to be approximately the site of the original transition between the northern and southern rhyolite sequences. Near the mouth of Byers Canyon, however, tuff beds of the basal composite unit lap over the fault, indicating that faulting occurred during the emplacement of this unit. There is thus a temporal relation between downfaulting of the basement and the first phase of rhyolitic volcanism in the central part of the Clan Alpine Mountains; moreover, the fault marks the boundary across which contemporaneous but remarkably different rhyolite sequences developed. The evidence suggests that the older rhyolite units of the southern sequence, interpreted previously to be of local origin, erupted in a faulted-bounded depression, most likely a volcano-tectonic feature. A thick assemblage of deposits derived from local sources accumulated in the depression.

The fault which cuts the earlier rhyolite units of the southern sequence at their southern boundary strikes northwesterly as does the fault at their northern margin discussed above. An hypothesis given earlier was that the fault which separates the earlier rhyolite units from the crystal tuff of Cherry Valley was the wall of a caldera which was filled by the crystal tuff unit at about 25 m.y. Thus, the two major faults in the southern rhyolite sequence are ostensibly similar responses to long-lived magma transfer.

It is important to obtain a figure of the actual depth to the bottom of the southern rhyolite sequence to understand the structure of this sequence as it applies to a volcano-tectonic theory of origin. Toward this end, G. A. Thompson of Stanford University has kindly provided simple Bouguer gravity values roughly in a northerly line between Bernice Canyon and Cherry Valley. Gravity station positions are on Figure 2, and a gravity profile is shown in Figure 6. Manual terrain corrections of Hammer zones d to m at the northernmost and southernmost stations are within 2 mgal, and it is assumed that terrain corrections at other stations are of similar values. Gravity measurements near Dyer Canyon are further corrected on Figure 6 for the effect of down-faulted low density materials just west at the range-front fault on the basis of other gravity data of Thompson (1971, written commun.) and refraction data of Meister (1967). Though the number of stations is sparse, the gravity values have grossly an arctangent distribution with an inflection near the boundary between the southern rhyolite sequence and the pre-Tertiary rocks and an amplitude of −30 mgal over the southern rhyolite sequence.

Figure 6 shows two model anomalies calculated as two-dimensional slabs of rhyolite with inclined northern edges by the method of Talwani and others (1959). The model parameters are depth of horizontal base of the southern rhyolite sequence and the density contrast of the rhyolite and pre-Tertiary rocks; model 1 is 4,000 m, 0.2 g/cc; model 2 is 2,000 m, 0.4 g/cc. Mesozoic rock densities in the Clan Alpine Mountains are 2.55 to 2.75 g/cc. Measured densities of the crystal tuff of Cherry Valley and dense rhyolites of the southern sequence are about 2.45 g/cc. The lacustrine and uncompacted tuffs are probably as low as 2.0 g/cc. Most of the exposed rocks of the southern sequence probably exceed 2.40 g/cc, and the quantity of exposed low density rock decreases south from the northern boundary of the southern sequence. Depths according to model 1 thus seem more likely than model 2. The principal uncertainty is whether densities of exposed rhyolite are representative of those at depth. Thus, the gravity models indicate basement depths increasing south to at least 2,000 m and most likely much deeper, perhaps 4,000 m, below the level of the exposed pre-Tertiary rocks (that is, 500 to 2,400 m below MSL). Taking the latter value as a depth limit, the elevation difference between the highest (2,700 m) and lowest (−2,400 m) levels in the ostensibly continuous southern rhyolite sequence indicates a maximum thickness of 5,100 m. Regardless of the uncertainties in density of the rhyolitic rocks and the sparse gravity data, the models indicate that the southern sequence is enormously thick compared to the northern sequence of ash-flow sheets and gives strong support to the proposition that the southern sequence accumulated in a depression, most likely akin to a caldera collapse.

REGIONAL CORRELATIONS

The differences between the northern and southern rhyolite sequences in the Clan Alpine Mountains and the tectonic features in the southern sequence are indicative of different geologic histories.

McKee and Stewart (1971) have tentatively correlated some of the ash-flow tuffs in the northern New Pass Range with those near Shoshone Creek in the Clan Alpine Mountains. The tuffs in both areas range in age from 22 m.y. to 30 m.y., with groupings at 28 to 30 m.y., 27 m.y., 24 to 25 m.y., and 22 m.y. The total duration of ash-flow tuff emplacement is the same as the range of ages of rhyolite in the southern Clan Alpine sequence, and individual eruptive times are also concurrent. Thick ash-flow deposits also occur in the northern Stillwater Range northwest of the Clan Alpine Mountains, and though we have no ages from the Stillwater rocks, they are likely to be partly contemporaneous with the northern Clan Alpine sequence.

South of the New Pass Range in the Desatoya Mountains, volcanic rocks change abruptly from thin stratified ash-flow sheets to poorly stratified, thick rhyolite beds which underlie most of the southern and central part of the range (Fig. 2); this change is remarkably like that seen in the Clan Alpine Mountains, although the rock units are not the same. Lithic units in the southern Desatoya Mountains are as yet incompletely delineated, but the range is dominated by a thick (1,200 m), densely compacted crystal tuff which is lithologically and structurally similar to the crystal tuff of Cherry Valley in the Clan Alpine Mountains and has the same age.

The north-south changes in Tertiary rhyolitic rocks in the New Pass–Desatoya Mountains that parallel those in the Clan Alpine Mountains suggest that the volcano-tectonic features of the southern sequence of the Clan Alpine Mountains are closely related to similar features in the Desatoya Mountains. These may represent a major east-trending geologic feature in west-central Nevada.

EVOLUTION OF THE VOLCANIC CENTER

Evidence that the southern Clan Alpine Mountains was the site of voluminous silicic volcanism between 24 and 30 m.y., and that the extrusion was concurrent with faulting and subsidence has been presented. The tectonism was probably related to caldera formation, but this feature has not yet been completely delineated. In addition, it seems clear that within the resolution of K-Ar dating, the two major eruptive episodes of the southern sequence of the Clan Alpine Mountains were contemporaneous with emplacement of many of the ash-flow sheets of the northern part of the range and correlative ash-flow sheets to the east and probably to the west. Such evidence by itself seems sufficient to propose that the source from which some of the widespread ash-flow sheets were erupted was in the southern Clan Alpine Mountains and perhaps southern Desatoya Mountains. A noteworthy exception is the 26 to 28 m.y.-old interval during which no eruptions are recognized in the southern sequence but during which several ash-flow tuffs were emplaced in the northern Clan Alpine and New Pass Mountains. A problem for future study is to determine whether such ash-flow sheets may also have been derived from the volcanic center of which the southern Clan Alpine sequence is a part, or whether they had sources elsewhere.

ACKNOWLEDGMENTS

Professor G. A. Thompson of Stanford University kindly provided Bouguer gravity values for the southern part of the Clan Alpine Mountains. These values have been used in our structural and tectonic analysis of the region. Mr. Max Budd performed eight of the chemical analyses presented in this paper. Some of the field work was supported by NSF Grant BA-1574, and some was done in cooperation with the Nevada Bureau of Mines on the Nevada State Map Project.

REFERENCES CITED

Blake, M. C., Jr., Hose, R. K., and McKee, E. H., 1969, Tertiary volcanic stratigraphy of White Pine County, Nevada: Geol. Soc. America, Abs. with Programs for 1969, pt. 5 (Rocky Mountain Sec.), p. 8.

McKee, E. H., and Silberman, M. L., 1970, Geochronology of Tertiary igneous rocks in central Nevada: Geol. Soc. America Bull., v. 81, p. 2317–2328.

McKee, E. H., and Stewart, J. H., 1971, Stratigraphy and potassium-argon ages of some Tertiary tuffs from Lander and Churchill Counties, central Nevada: U.S. Geol. Survey Bull. 1311-B, p. B1–B28.

Meister, L. J., 1967, Seismic refraction study of Dixie Valley, Nevada: U.S. Air Force Cambridge Research Labs. Spec. Rept. 66–848, pt. 1.

O'Connor, J. T., 1965, A classification for quartz-rich igneous rocks based on feldspar ratios: U.S. Geol. Survey Prof. Paper 525–B, p. 79–84.

Riehle, J. R., 1970, Theoretical compaction profiles of ash-flow tuffs [Ph.D. thesis]: Evanston, Illinois, Northwestern Univ.

Speed, R. C., and Jones, T. A., 1969, Synorogenic quartz sandstone in the Jurassic mobile belt of western Nevada—Boyer Ranch Formation: Geol. Soc. America Bull., v. 80, p. 2551–2584.

Talwani, M., Worzel, J. L., and Landisman, M., 1959, Rapid gravity computations for two-dimensional models with application to the Mendocino Submarine Fracture Zone: Jour. Geophys. Research, v. 64, p. 49–59.

Yoder, H. S., Jr., 1969, Calcalkalic andesites—experimental data bearing on the origin of their assumed characteristics, *in* McBirney, A. R., ed., Proceedings of the Andesite Conference: Oregon Dept. Geology and Mineral Industries Bull. 65, p. 77–89.

MANUSCRIPT RECEIVED BY THE SOCIETY JULY 21, 1971

REVISED MANUSCRIPT RECEIVED NOVEMBER 29, 1971

MBERG

mples to 60 kb and 1000°C, ...s Lab., Kirkland Air Force ..., 2nd Quarterly Rept., Apr...

Experimental study of the ..., Bull. Geol. Soc. Am., 67, ...

...ts of shock pressures from a ... on mechanical and optical ...diorite, J. Geophys. Res., 71, ...

...d E. M. Lilley, Static P... and consolidated earth mate... Univ. Calif. Lawrence Radia... UCRL-14711, March 1966.
Strength experiments under ... Z. Ver. Deut. Ing., 55, 174..., ...llected Works of Theodore ... 1, pp. 274–303, Butterworths ...ions, London, 1956. In Ger...

...ffects of cracks on the com... k, J. Geophys. Res., 70, 381, ...

...ed July 7, 1967;
...ptember 14, 1967.)

Dixie Valley, Churchill Co. Area

JOURNAL OF GEOPHYSICAL RESEARCH VOL. 73, NO. 4 FEBRUARY 15, 1968

Aeromagnetic Measurements in Dixie Valley, Nevada; Implications on Basin-Range Structure

THOMAS E. SMITH[1]

Geophysics Department, Stanford University, Stanford, California 94305

Interpretation of an aeromagnetic survey flown during 1964 suggests that the pre-Tertiary magnetic basement under Dixie Valley, Nevada, forms an asymmetric composite graben whose inner block is approximately 5 km wide and lies under the western half of the valley at an average depth of 1.9 km. Steplike 'shelf' blocks bordering the narrow inner graben are also downthrown with respect to adjacent ranges, but to a lesser degree; the western shelf is approximately 300 meters below the surface, whereas the eastern conjugate block lies about 500 meters below the surface. The average depth of valley fill across the composite graben is approximately 765 meters. Depth estimates imply, in addition, that the eastern shelf block is broken by several NW-trending transverse faults of 300- to 600-meters displacement. The magnetic expression of contacts between a Jurassic gabbroic complex and other basement rocks can be traced across both northern and southern Dixie Valley. An absence of appreciable horizontal offset of this contact across most of the major Basin-Range faults indicates that post-Jurassic displacements have been primarily dip-slip. An apparent right lateral offset of 2–3 km may exist along the eastern side of the deepest graben block, however. Models computed from anomalies over the southern gabbro contact tend to verify earlier geologic inferences that this intrabasement complex is of lopolithic form. The apparent northward displacement of the gabbro outcrops and contact in the Clan Alpine Range from the subsurface position of gabbroic basement in eastern Dixie Valley may reflect an uplift of the range, relative to the valley block, with subsequent erosional stripping of the tapered lopolith. Satisfactory alternative solutions of an equidimensional anomaly in southeastern Dixie Valley are either a volcanic cone or an equidimensional volcanic remnant. Both computational models overlie the gabbroic complex and require a high total magnetization.

INTRODUCTION

Dixie Valley and the adjacent mountain ranges considered in this paper are located in the western part of the Basin and Range structural province and are bounded approximately by latitudes 39°20′N and 40°15′N and by longitudes 117°30′W and 118°30′W (Figure 1).

Since the earthquake of December 16, 1954, Dixie Valley and the surrounding areas have been the foci of numerous investigations. Effects of that dynamic display of tectonic activity and the availability of supplementary information contributed by investigators in the various disciplines renders Dixie Valley particularly advantageous for geophysical studies of Basin and Range structural problems.

Magnetic data were collected in Dixie Valley during 1964 for determining the structural history and subsurface geometry of that basin. Of primary concern in this investigation was the establishment and tracing, by means of magnetic measurements, of a geologic contact intersected by the major fault systems of Dixie Valley. The magnetic expression of displacements on this contact establishes whether shallow crustal faulting throughout the Cenozoic era has been principally of a normal sense, as the 1954 scarps and strain data suggest [*Slemmons*, 1957, and L. J. Meister, personal communication, 1966], or, alternatively, movement in a strike-slip sense has been of significance [*Sales*, 1966; *Romney*, 1957].

A secondary objective was to examine, through gradient analyses, the general configuration of magnetic basement under Dixie Valley, both as an aid to programming subsequent seismic refraction work and as a means of extrapolating between seismic profiles. An additional aspect, investigated through computational models, was the intrabasement geometry of a gabbroic complex exposed in adjacent mountain ranges.

Previous geological work in Dixie Valley and

[1] Now at Mackay School of Mines, University of Nevada, Reno, Nevada 89507.

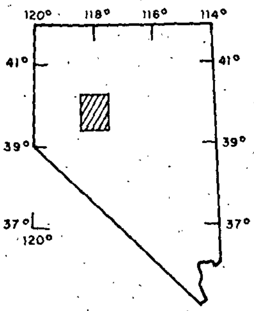

Fig. 1. Index map of Nevada showing location of the Dixie Valley area.

adjacent mountains has been primarily concerned with surface mapping, subsurface studies being limited to hydrologic investigations from shallow well data [*Cohen et al.*, 1963]. The stratigraphy and structure of the extreme north end of the project area have been discussed by *Muller et al.* [1951]. Of particular value to the present project has been recent mapping of the Stillwater Range and parts of the West Humboldt and Clan Alpine ranges by *Page* [1965] and *Speed* [1963]. Previous geophysical studies in and near the region of interest have been limited to a gravity survey of Dixie Valley [*Thompson*, 1959, and unpublished], a recent gravity survey of the Carson Sink–West Humboldt area [*Wahl*, 1965], a complete geological geophysical investigation of the Sand Springs Range, Fairview Valley, and Fourmile Flat area to the south of Dixie Valley [*Nevada Bureau of Mines*, 1963], and seismological investigations of the December 1957 earthquakes [*Romney*, 1957; *Cloud*, 1957].

Collection and Reduction of Data

Magnetic total intensity measurements were taken with a Varian model M-49 nuclear precession magnetometer adapted for aeromagnetic use. The instrument package, mounted in a light aircraft, was connected through 31 meters of suspension and transmission line to the sensing unit. It was found that this cable length effectively eliminated magnetic interference of the airplane, regardless of flight orientation. Actuation of the polarization to readout cycle was effected manually by an operator at 10-sec intervals determined by a stop watch. Station values accurate to ±5 gammas and pertinent location information were recorded by a third person in the aircraft.

Positioning of flight lines was controlled by establishing a series of ground reference points over which the pilot would fly, indicating to the recorder when these points were crossed. In the subsequent plotting of data, station points were linearly distributed between reference locations, compensating for variations in ground speed. Locations accurate to approximately ±100 meters were established by this method. With minor exceptions, flight lines were flown at a barometric elevation of 1280 ±15 meters above sea level. This elevation corresponds to an approximate height of 215 meters above the valley floor. Departures from this elevation were necessary only over isolated alluvial fans at the basinal margin.

During periods of aeromagnetic measurement, a continuous monitor of total intensity was recorded by Varian Associates in Palo Alto, California (37°30′N, 122°05′W). Diurnal and transient variations appearing on those records were compensated for in all survey data.

A linear gradient of 1.2 gammas/km in the direction N 30°E was assumed as a regional corrective factor for all magnetic data [*U. S. Coast and Geodetic Survey*, 1955]. After application of space and time dependent corrections, crossing profiles generally agreed to within 15 gammas. This value closely approaches the inherent standard deviation error in the survey, and, in view of the 50-gamma map contour interval desired, no further statistical adjustments were made to data within the survey grid.

Generalized Geology and Magnetic Units

A comparison of the mapped geology (Figure 2) with a magnetic profile flown along the crest of the Stillwater Range (Figure 3) and with the total intensity isoanomalic map of Dixie Valley (Figure 4) reveals that the numerous rock units mapped by *Page* [1965] and *Speed* [1963] in that and other ranges form three principal magnetic mega-units. The southernmost of these includes sedimentary rocks of Upper Triassic age and overlying welded tuffs, latite, and rhyolite. An average total intensity anomaly over this unit is approximately 200 gammas above the magnetic base level of 53,150 gammas observed in the area farther south [*U. S. Coast and Geodetic Survey*, 1955]. Bordering these rocks on the north, a second magnetic unit, of late Jurassic age, is composed of heterogeneous

lines was controlled by
ground reference points
would fly, indicating to
se points were crossed. In
ng of data, station points
ed between reference loca-
for variations in ground
curate to approximately
tablished by this method,
ns, flight lines were flown
tion of 1280 ±15 meters
elevation corresponds to
of 215 meters above the
ures from this elevation
over isolated alluvial fans

eromagnetic measurement,
of total intensity was re-
ociates in Palo Alto, Cali-
05'W). Diurnal and tran-
ring on those records were
ll survey data.
of 1.2 gammas/km in the
as assumed as a regional
all magnetic data [*U. S.*
urvey, 1955]. After appli-
ime dependent corrections,
rally agreed to within 15
closely approaches the in-
ation error in the survey,
0-gamma map contour in-
her statistical adjustments
ithin the survey grid.

GY AND MAGNETIC UNITS

e mapped geology (Figure
rofile flown along the crest
ge (Figure 3) and with the
malic map of Dixie Valley
that the numerous rock
[1965] and *Speed* [1963]
nges form three principal
The southernmost of these
rocks of Upper Triassic
welded tuffs, latite, and
total intensity anomaly
proximately 200 gammas
ase level of 53,150 gammas
farther south [*U. S. Coast*
, 1955]. Bordering these
second magnetic unit, of
omposed of heterogeneous

gabbroic intrusive rocks and basalt, which generate a strongly undulatory anomaly averaging approximately 500 gammas. The third magnetic unit of significance, unexposed in the ranges, borders the aforementioned gabbroic suite on the north. The magnetic expression of this mega-unit, of comparable magnitude but lower relief, suggests it is more homogeneous than the gabbroic complex.

Triassic rocks of the southern magnetic unit in the Stillwater Range are exposed generally south of latitude 39°50'N. They occur as gray-black, grayish weathering slates and phyllites. Over the greater part of the exposure, only incipient recrystallization is evident, although exceptions do occur near granite contacts. Complex deformation of these rocks precludes direct measurement of their thickness; however,

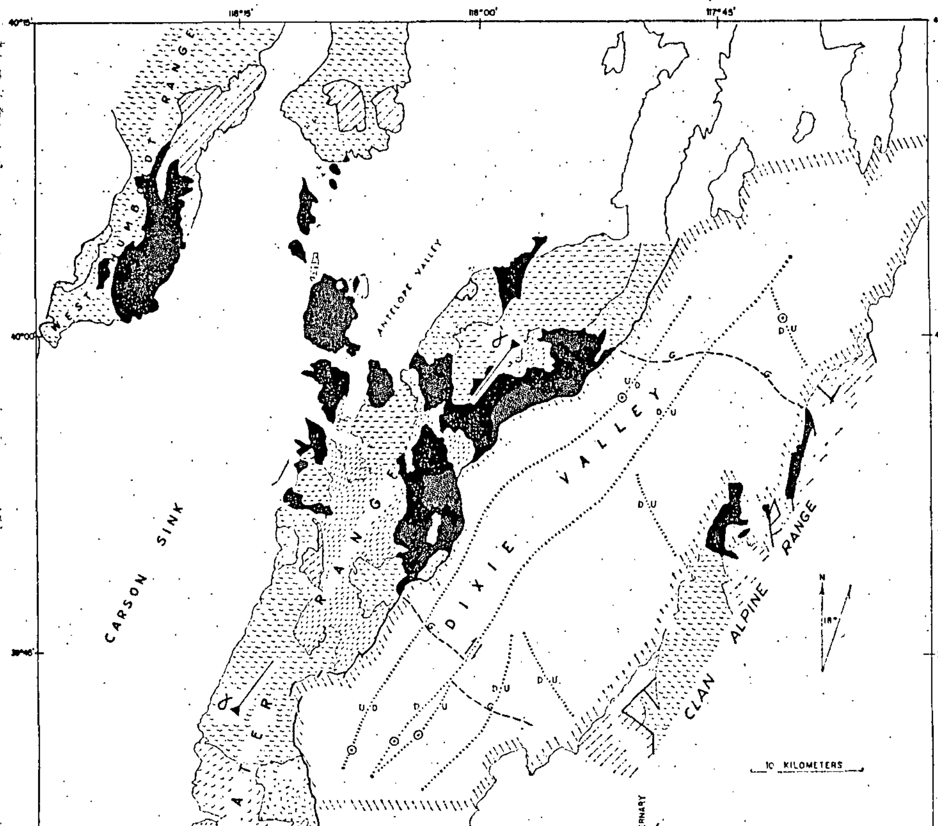

Fig. 2. Generalized geologic map of the West Humboldt, Stillwater, and Clan Alpine ranges, Nevada. Surface geology adapted from *Page* [1965] and *Speed* [1963]. Subsurface structures inferred from geophysical data. α–α' denotes location of section shown in Figure 3.

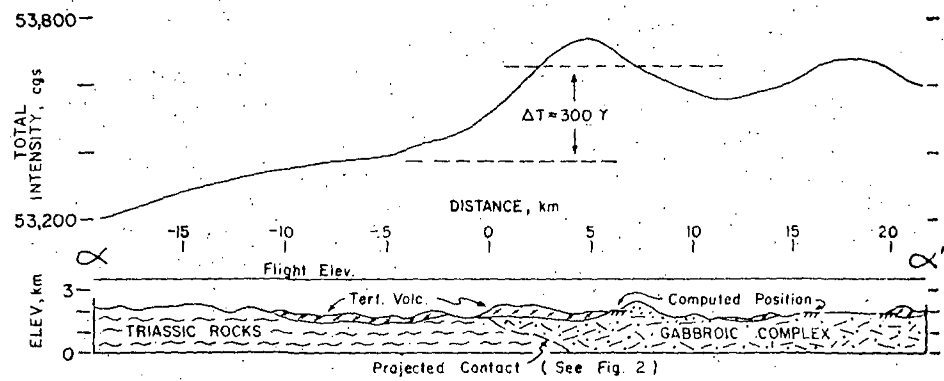

Fig. 3. Generalized geologic section and observed total intensity anomaly along the Stillwater Range, Nevada, between α and α' of Figure 2.

estimates are between 1500 and 3000 meters [*Page*, 1965]. Fossils collected in this marine unit indicate that it is of Upper Triassic age.

South of latitude 39°40'N, the Triassic slates are unconformable overlain by a number of magnetically similar volcanic units. They are shown as undifferentiated devitrified welded tuffs, rhyolite, and latite on Figure 2. Of nonmarine origin, these rocks may range in age from Late Jurassic through early Tertiary. The composite thickness of this sequence is as much as 4800 meters [*Page*, 1965].

The second magnetic mega-unit is exposed north of latitude 39°50' in the Stillwater Range. Intrusive rocks of this unit form a heterogeneous gabbroic assemblage, which includes diorite, gabbro, picrite, anorthosite, diabase, keratophyre, and gabbroic pegmatite. Along margins of the intrusion, differentiation layering has been noted. A potassium-argon age determination from similar rocks in the West Humboldt Range indicates the complex is probably of Late Jurassic age [*Speed*, 1962*a*, *b*]. Closely associated with the intrusive gabbroic complex are large areas of altered basalt that appear to be co-genetic and perhaps contemporaneous with the intrusive suite. Speed suggests that the entire complex, of lopolithic form, was emplaced at shallow depth, locally erupting to form the associated effusives.

Along much of the Stillwater crest, the gabbroic unit is capped by Tertiary flows and pyroclastics of rhyolite, dacite, latite, and andesite. Dissection of the flows exposes a total thickness of about 550 meters. Approximating a thin plate geometry, these rocks exhibit an apparent magnetic transparency.

In Dixie Valley proper, as in many other valleys of the western Basin and Range, great thicknesses of late Cenozoic lake and stream deposits have accumulated. They range in age from Pliocene to Recent and include alluvial fan detritus, channel deposits, and lacustrine sediments. For the most part, the lake sediments consist of silt and clay, although shoreline deposits of gravel and sand exist locally. For the purpose of this investigation, complexities in this sequence are ignored; it is considered as essentially nonmagnetic valley fill.

Determination of Magnetic Parameters

To assign representative parameters to the various magnetic units, methods of approach were employed that depend both on inferences derived from total intensity profiles and on individual rock samples from the region. A limited number of samples were collected by the writer and by R. C. Speed from the Clan Alpine, West Humboldt, and Stillwater ranges. From cores of these specimens, volume susceptibility, magnitude of remanent magnetization, and density were determined (Appendix). High average values of remanence, particularly in the gabbroic complex, dictated the application of methods that consider that property. The general method adopted has its basis in techniques, discussed by *Green* [1960] and *Hays and Scharon* [1963], that established an *equiva-*

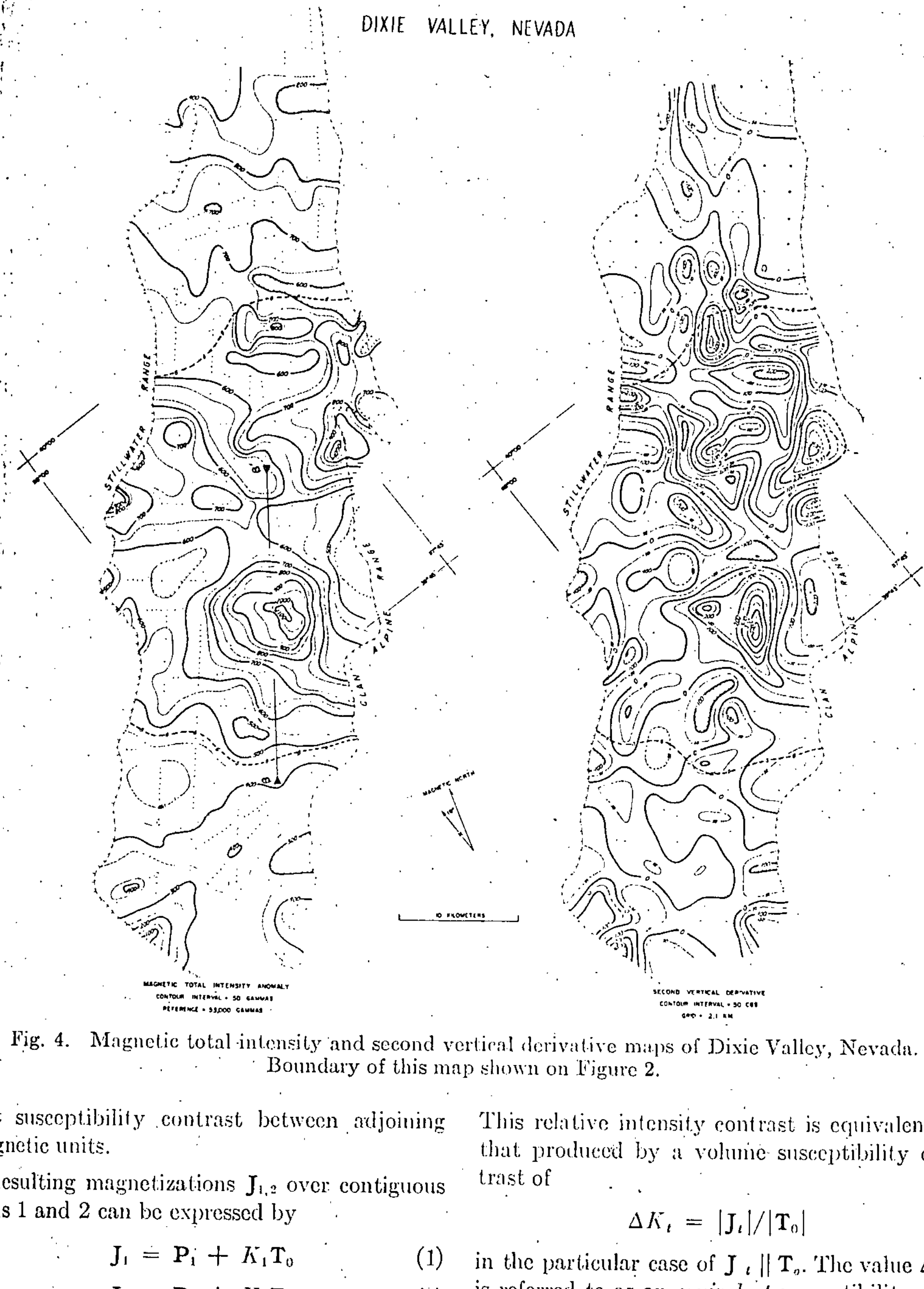

Fig. 4. Magnetic total intensity and second vertical derivative maps of Dixie Valley, Nevada. Boundary of this map shown on Figure 2.

ent susceptibility contrast between adjoining magnetic units.

Resulting magnetizations $\mathbf{J}_{1,2}$ over contiguous units 1 and 2 can be expressed by

$$\mathbf{J}_1 = \mathbf{P}_1 + K_1\mathbf{T}_0 \quad (1)$$

$$\mathbf{J}_2 = \mathbf{P}_2 + K_2\mathbf{T}_0 \quad (2)$$

where K is the volume susceptibility, $\mathbf{P}$ is the remanent magnetization, and $\mathbf{T}_0$ is the geomagnetic field intensity. A relative contrast of magnetization is then given by

$$\mathbf{J}_t = (\mathbf{P}_1 - \mathbf{P}_2) + (K_1 - K_2)\mathbf{T}_0 \quad (3)$$

This relative intensity contrast is equivalent to that produced by a volume susceptibility contrast of

$$\Delta K_t = |\mathbf{J}_t|/|\mathbf{T}_0| \quad (4)$$

in the particular case of $\mathbf{J}_t \parallel \mathbf{T}_0$. The value ΔK_t is referred to as an *equivalent* susceptibility contrast.

Application of this expression in the present study assumes that remanent components of magnetization in all units are parallel to the present inducing field and, further, that reversal of permanent components is not of importance in the area of interest. These assumptions are necessary in the absence of detailed paleomagnetic sampling. In addition, the Triassic slate is assumed to have negligible remanence. With these constraints on the method, equation 3 becomes

$$\mathbf{J}_t = \mathbf{P}_{gb} + (K_{gb} - K_{so})\mathbf{T}_0 \qquad (5)$$

where the subscripts *gb* and *so* refer to the gabbroic and southern magnetic units, respectively.

Using only the average anomaly over the magnetic units, we can establish a lower limiting value of either K or ΔK by means of the following expressions [*Reford*, 1964]:

$$K_t = \Delta \mathbf{T}/2\pi \mathbf{T}_0 \sin^2 i \qquad (6a)$$

$$\Delta K_t = \Delta \mathbf{T}/2\pi \mathbf{T}_0 \sin^2 i \qquad (6b)$$

where i is field inclination. Equation 6*a* determines a minimum *equivalent* susceptibilty over an infinite magnetic basement, whereas equation 6*b* provides a minimum *equivalent* susceptibility contrast between two semi-infinite magnetic bodies of differing magnetizations. The former was used in this investigation to determine a value of $K_{so} = 700 \times 10^{-6}$ cgs for the southern magnetic mega-unit. Because this value clearly represents a minimum, a K_{so} value of 1000×10^{-6} cgs was assumed for calculation of an *equivalent* contrast between the southern magnetic unit and the gabbroic complex. Insertion of this K_{so} value and an average of measured gabbro susceptibility and remanence (Appendix) into (5) yields $K_{gb-so} = 2700 \times 10^{-6}$ cgs.

If equation 6*b* and a $\Delta \mathbf{T}$ value of 300 gammas (Figures 3 and 6) are used to determine K_{gb-so}, a minimum value of 1050×10^{-6} cgs is obtained. The best value of K_{gb-so} most probably falls between this value and the value determined from the rock sample analyses; model computations in this investigation assume, therefore, an *equivalent* susceptibility contrast of 2500×10^{-6} cgs across this contact.

Interpretation of Magnetic Data

Qualitative inferences. Dominating the center of the total intensity map is a broad region of sharp anomalies exhibiting numerous closures of high magnetic relief. General characteristics or 'fabric' and dipolar effects of this zone are even more discernible through an appropriate second vertical derivative filter (Figure 2). It should also be noted that the average magnetic base level over this region is approximately 300 gammas higher than over the adjoining area south of 39°45'N (Figure 3 and 4). The southernmost margin of this undulatory magnetic 'plateau' is marked by a linear gradient trending N 45°W at this latitude. Where the inflection line of this gradient intersects the Stillwater Range, it is nearly coincident with the mapped exposures of the gabbroic complex, suggesting that the high average level and magnetic topography to the north are correlative with the complex. Additional evidence of this correlation is furnished by a profile flown along the crest of the Stillwater Range, where a similar shift in magnetic level over the southern gabbroic edge is noted (Figure 3). Figures 2 and 4 show the position of the gradient inflection and inferred gabbro boundary across Dixie Valley.

Control on position of the northern contact of the complex is less exact in that a comparable shift in magnetic level is not observed. An approximate boundary can be established, however, by correlating the northernmost extent of the undulatory magnetic province with exposures of gabbro in adjacent mountains. A line indicating the inferred position of the contact trends roughly S 80°E from latitude 40°00' in the Stillwater Range.

Extending northeasterly along the axis of Dixie Valley is a longitudinal, linear trend of anomalies of relatively high amplitude. To the west, approximately 4 km from and parallel to the east flank of the Stillwater, is a second elongate anomalic trend, which is more subdued than the first. Along these longitudinal zones, most prominent crosstrends are truncated or deflected. Coincidence of several such anomalies and their amplified counterparts on the filtered map with faults located by seismic refraction [*Meister*, 1967] implies that they may be edge effects over major subsurface fault systems. Both seismically determined locations and extrapolations of the faults are shown on Figure 2. By this interpretation, the basement under Dixie Valley is suggestive of a composite, asymmetric graben whose deepest inner block is about 5 km wide and lies under the western half of the valley. Steplike 'shelf' blocks border-of the narrow inner graben are downthrown with respect to adjacent ranges, but to a lesser degree.

In addition to the longitudinal trends, several transverse anomalies other than those discussed earlier are in evidence. They are located for the most part over the eastern shelf and trend obliquely (N 25°W) to the major features. Depth estimates on this block and coincidence with projections of faults in the Clan Alpine Range provide two lines of evidence that these anomalies are expressions of transverse faulting.

There is little magnetic indication of large strike-slip displacements along the longitudinal fault systems of Dixie Valley. This is particularly true along the western bounding fault of the valley, where no appreciable offset is noted between the aforementioned magnetic inflection line and mapped exposures of the gabbroic complex, implying that post-gabbroic displacements (since Late Jurassic) have been primarily, if not entirely, of a normal sense.

Along the central fault zone, exceptions to this generality do exist; there, several anomalies of transverse strike are deflected 2 to 3 km in a right lateral direction (Figures 2 and 4).

Basement topography. In magnetic studies of sedimentary basins, techniques of depth estimation are generally employed in order to establish basement configuration. Most such methods operate on magnetic gradients and are usually independent of rock parameters, requiring only that they remain constant within the assumed geometric model. For the reconnaissance purpose of this study and in view of the numerous dike-like bodies exposed in the neighboring ranges, the method of *Peters* [1949] was adopted for applicable profiles in Dixie Valley. The factor by which Peters' 'half-slope' index is converted to depth was empirically determined from a control profile over the Stillwater Range; a value of 1.35 was found to give representative depths along the entire profile (Figure 3).

Applying Peters' expression to depth indices from profiles parallel to usable gradients, it was possible to construct a topographic map of the magnetic basement (Figure 5). Most striking of the features revealed by this map is a longitudinal trough whose axis is approximately 6 km from and parallel to the Stillwater Range. Close spacing of depth contours along the edges of the trough lends confirmation to the fault-bounded graben mentioned above. Both the longitudinal anomalic trends and seismic fault locations fall within these closely spaced contours (Figures 4 and 5). This interpretation

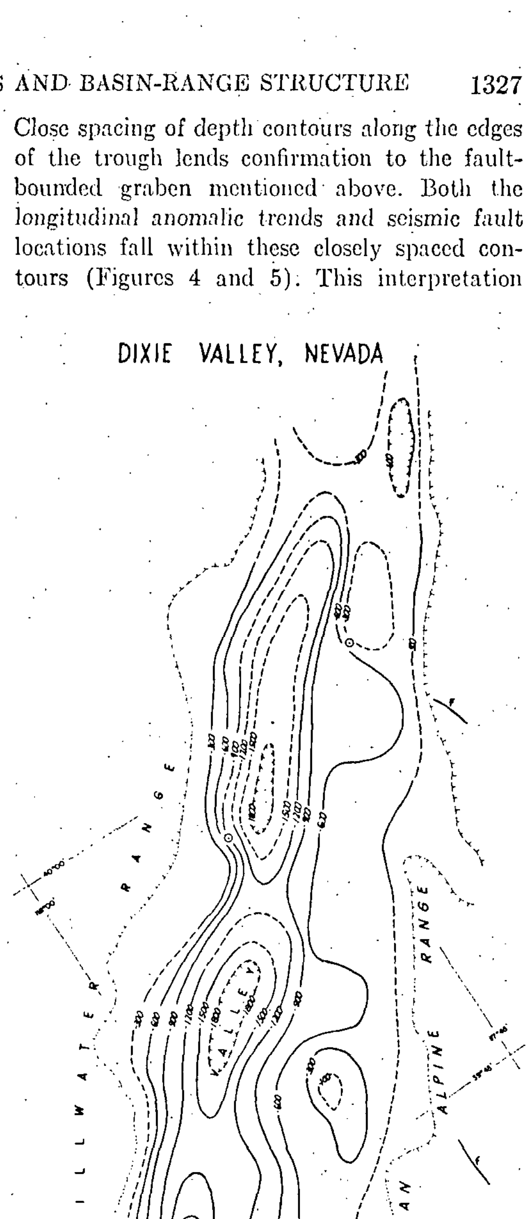

Fig. 5. Topographic map of magnetic basement (compiled from depth estimates).

agrees well with those determined independently from gravity analysis (G. A. Thompson, unpublished) and by seismic refraction studies [*Meister*, 1967].

An average of depths taken at the intersections of a 2-km grid superimposed over this map indicates that the average depth of magnetic basement across Dixie Valley is approximately 765 meters. This places the mean level of the basin floor at an elevation of 335 meters above sea level. Only the narrow inner graben, underlying much less than half the total surface area of the valley, is depressed below sea level.

Secondary features of significance on this map are the apparent transverse 'steps' in the eastern half of the valley. The most northerly of these steps trends approximately N 30°W and displays 300 to 600 meters of vertical offset. A similar deflection of depth contours is present about 20 km to the southwest, suggesting a second transverse fault with displacement in

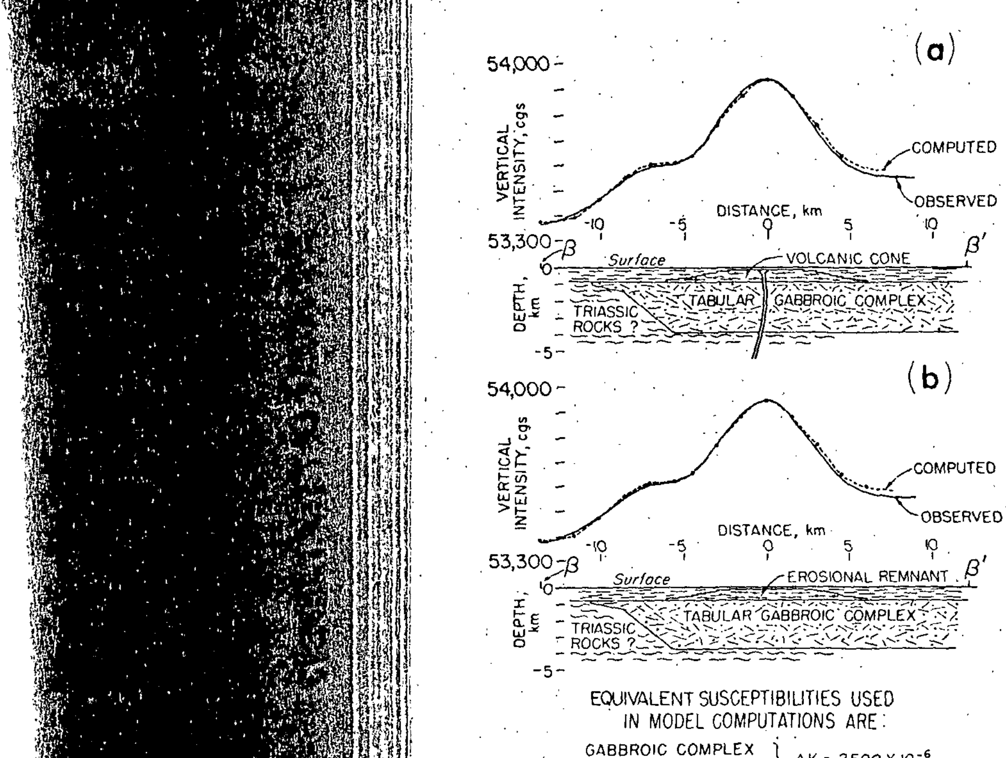

Fig. 6. Alternative solutions satisfying equidimensional anomaly in southeastern Dixie Valley. (*a*) A buried volcanic cone model. (*b*) An erosional remnant model.

the same sense but of approximately 300 meters.

Finally, the basement map clearly delineates a roughly equidimensional high in the southeast part of Dixie Valley, which coincides precisely with a closed magnetic high of 500 gammas. Application of the depth expression to the extremely steep gradients over this feature indicates its top is between 60 and 150 meters below the valley surface. A comparable depth was subsequently obtained by seismic refraction [*Meister*, 1967]. Total relief of the 'buried mountain' above the mean level of the eastern valley block is roughly 600 meters.

Model representations of the magnetic units. A secondary objective of this investigation was to test a hypothesis offered by Speed, who, on the basis of detailed surface mapping, has suggested the gabbroic complex forms an elongate northwest-trending body of lopolithic form (R. C. Speed, oral communication, 1964). To investigate this possibility, a computational analysis of a N–S profile ($\beta\beta'$ on Figures 4 and 6) over the southern edge of the complex was performed using a Pirson graticule integrator for two-dimensional bodies [*Pirson*, 1940]. Utilizing the previously calculated susceptibility contrast for this contact, a series of successive model assumption–curve comparison operations yielded the tabular model shown in Figure 6. The associated intensity curve over this model accords well with the two-dimensional component of the observed anomaly.

Existence of such a tabular body is further substantiated by indirect indications on the east side of Dixie Valley. There, the magnetic expression of the subsurface contact is over 20 km southwest of the nearest surface exposure (Figure 2). Strike-slip movement could produce a left-lateral displacement of this magnitude, although it may equally well be attributed to Clan Alpine uplift and subsequent erosional stripping of a lopolithic body. The latter interpretation is preferred by the author in view of the dip-slip or right lateral strike-slip movements exhibited by the other Basin and Range faults in the basin. An unlikely probability would be required, in addition, to explain the exact coincidence of subsurface and surface gabbro contacts observed in northeastern Dixie Valley, if strike-slip movements had occurred along the eastern border of the valley. If it is assumed that the gabbroic complex is of lopolithic form, a northward extrapolation of the lower gabbro contact shown in Figure 6 would place the depth between 3 and 5 km, implying a relative Clan Alpine uplift of comparable magnitude to produce the apparent offset.

A second investigative approach was used to study the dominant magnetic 'high' in southeastern Dixie Valley. For purposes of computation, the three-dimensional component of profile $\beta\beta'$ (Figures 4 and 6) was smoothed and reduced to vertical intensity amplitude. The resulting curve is similar to the anomaly induced by a vertical field except for the usual asymmetry of total intensity at this geomagnetic latitude, i.e., a slight southward migration of the maximum and a discernible minimum on the north. At this magnetic latitude, the peak migration of either a point pole or a point dipole is only of the order of tens of meters [*Smellie*, 1956], a negligible quantity when compared to the observed anomaly width of 12 km. As a consequence, reduction to vertical intensity, although introducing no appreciable error in solution, facilitates the use of solid angle charts developed by Nettleton for determining magnetic effects of buried vertical cylinders [*Nettleton*, 1942].

Three-dimensional models depicted in Figure 6 with associated *equivalent* susceptibilities are constructed of superposed vertical cylinders. Either model generates magnetic effects that are in close agreement with the reduced observed anomaly. Figure 6*a* attributes the equidimensional anomaly to a volcanic cone of high permanence and consequent *equivalent* susceptibility, whereas Figure 6*b* represents an erosional volcanic remnant with similar total magnetization. The *equivalent* susceptibilities indicated for these models are the ones necessary to satisfy the reduced anomaly. The feeder in Figure 6*a* is assumed to contribute a negligible magnetic effect. Both models are in reasonable agreement with gravity and seismic measurements in this area [G. A. Thompson, unpublished; *Meister*, 1967].

Summary of Conclusions

This investigation supports the interpretation that basement rocks under Dixie Valley form a composite asymmetric graben, which is roughly parallel to the valley axis. The inner graben block is approximately 5 km wide and lies under the western half of the valley at an average depth of 1.9 km. In spite of the extreme depth of this narrow feature, however, the average depth of magnetic basement under Dixie Valley is only 765 meters below the present surface. Between the main graben and the bordering mountain ranges are shelf blocks, also downthrown with respect to the ranges but to a smaller extent. The eastern shelf is broken by a series of NW-trending normal faults with smaller displacements. This general configuration is in basic agreement with seismic refraction studies and gravity measurements in the area.

The contacts of an intrabasement gabbroic complex can be traced across both northern and southern Dixie Valley. No appreciable strike-slip displacements of the southern contact are in evidence, except along the eastern side of the inner graben, where a maximum offset of 2–3 km may be present. This implies that post-Late Jurassic movements on the major fault systems have been primarily dip-slip. It is suggested that dip-slip movement on a conical fault surface is responsible for minor en echelon structures observed at the surface.

A model computed from the anomaly over the southern gabbro contact lends confirmation to an earlier suggestion that the gabbroic complex is of lopolithic form. If a body similar to the computational model is vertically displaced on a Basin and Range fault, an apparent horizontal offset of the contact may result. This mechanism is suggested to explain the apparent gabbro offset along the eastern side of Dixie Valley and requires a relative dip-slip displacement of 3 to 5 km.

Additional computational models suggest the three-dimensional anomaly in southeastern Dixie Valley may be generated by a volcanic cone or, alternatively, by an equidimensional volcanic remnant; either model requires a high *equivalent* susceptibility.

Acknowledgments. I am indebted to Sheldon Breiner of Varian Associates for the use of a magnetometer and for monitoring of total intensity background. Dr. R. C. Speed of the Jet Propulsion Laboratory has been extremely helpful in providing an additional magnetometer; both he and Dr. Ben M. Page of Stanford University have generously contributed geologic information on the mountain ranges adjacent to Dixie Valley. Sincere

APPENDIX. PHYSICAL PROPERTIES OF ROCK SAMPLES

Sample	Rock Type	Volume Susceptibility, cgs Units $K \times 10^6$	Permanent Magnetization, cgs Units $\|P\| \times 10^4$	Density, g/cc
	Southern Magnetic Mega-Unit			
1	Latite	100	1.76	2.51
2	Latite	910	0.00	2.49
3	Welded tuff	930	58.1	2.57
	Average	646	20.0	2.52
	Gabbroic Complex			
4	Gabbro	2910	31.2	2.82
5	Gabbro	4120	21.9	2.74
6	Gabbro	680	17.3	2.82
7	Gabbro	160	0.017	2.87
8	Diabase	3570	9.79	2.81
9	Scapolitized gabbro	3330	3.94	2.70
10	Gabbro	40	0.173	2.82
11	Albitized gabbro	20	0.028	2.71
12	Anorthosite	1130	2.00	2.67
13	Peridotite	2790	12.5	2.99
14	Altered gabbro	3700	12.6	2.87
15	Hydrated basalt	420	2.22	2.71
	Average	1906	9.47	2.79

gratitude is expressed to the late Professor J. L. Soske and to Professor G. A. Thompson for their counsel and suggestions.

REFERENCES

Cloud, William K., Intensity distribution and strong-motion seismograph results, Nevada earthquakes of December 16, 1957, *Bull. Seismol. Soc. Am., 47,* 327, 1957.

Cohen, Philip, and D. E. Everett, A brief appraisal of the ground-water hydrology of the Dixie-Fairview Valley area, Nevada, *Dept. Conserv. Nat. Res., State of Nevada, Rept.* 23, 1963.

Green, R., Remanent magnetization and the interpretation of magnetic anomalies, *Geophys. Prospecting, 8,* 88, 1960.

Hays, W. W., and L. Scharon, An example of the influences of remanent magnetization on magnetic intensity measurements, *Geophysics, 28,* 1037, 1963.

Meister, L. J., Seismic refraction study of Dixie Valley, Nevada, *A. F. Cambridge Res. Lab. Final Sci. Rept. AFCRL-66-848,* part 1, 1967.

Muller, S. W., H. G. Ferguson, and R. J. Roberts, Geology of the Mt. Tobin quadrangle, Nevada, *U. S. Geol. Surv. Geol. Quad. Map GQ-7,* 1951.

Nettleton, L. L., Gravity and magnetic calculations, *Geophysics, 7,* 293, 1942.

Nevada Bureau of Mines and Desert Research Institute, Geological, Geophysical, chemical, and hydrological investigations of the Sand Springs Range, Fairview Valley, and Fourmile Flat, Churchill County, Nevada, *U. S. Atomic Energy Comm., Div. Tech. Inf., Vela Uniform Prog., Proj. Shoal, Final Rept. VUF-1001,* 1963.

Page, Ben M., Preliminary geologic map of a part of the Stillwater Range, Churchill County, Nevada, *Nev. Bur. Mines Map 28,* 1965.

Peters, L. J., The direct approach to magnetic interpretation and its practical application, *Geophysics, 14,* 290, 1949.

Pirson, S. J., Polar charts for interpretation of magnetic anomalies, *Trans. Am. Inst. Mining Met. Engr., 138,* 173, 1940.

Reford, M. S., and J. S. Sumner, Aeromagnetics, A review article, *Geophysics, 29,* 482, 1964.

Romney, C., Seismic waves from the Dixie Valley-Fairview Peak earthquake, *Bull. Seismol. Soc. Am., 47,* 301, 1957.

Sales, John K., Structural analysis of the Basin-Range province in terms of wrench faulting, Ph.D. dissertation, University of Nevada, Reno, 1966.

Slemmons, D. B., Geological effects of the Dixie Valley-Fairview Peak, Nevada, earthquakes of December 16, 1954, *Bull. Seismol. Soc. Am., 47,* 353, 1957.

Smellie, D. W., Elementary approximations in aeromagnetic interpretation, *Geophysics, 21,* 1021, 1956.

Speed, R. C., Humboldt gabbroic complex (abstract), *Geol. Soc. Am. Spec. paper 73,* 1962*a*.

Speed, R. C., Scapolitized gabbroic complex, West Humboldt Range, Nevada, Ph.D. thesis, Stanford University, Stanford, Calif., 1962*b*.

Speed, R. C., Unpublished progress map in parts of the West Humboldt, Stillwater, and Clan Alpine Ranges, Nevada, 1963.

Thompson, G. A., Gravity measurements between Hazen and Austin, Nevada, A study of Basin-and-Range structure, *J. Geophys. Res., 64,* 217, 1959.

U. S. Coast and Geodetic Survey, Total intensity chart of the United States, 1955.

Wahl, R. R., An interpretation of gravity data from the Carson Sink area, Nevada, M.S. Research Project, Stanford University, Stanford, Calif., 1965.

(Received June 12, 1967.)

Dixie Valley
Churchill Co

1973, Flow of
iuea Volcano,
, v. 84, no. 2,
A. R., 1970,
nd terrestrial
nge: Science,
c, J. G., 1966,
t in Alae lava
. 29, p. 629-
969, Thermal
Am. Geophys.
9.
mik lebender
v. 8, no. 3, p.
basalt in the
v. 10, p. 510-
ipply rate at
cience, v. 175,
., 1972, Partial
: of Alae lava
Geol. Survey
ackson, D. B.,
The complex
iuea Volcano.
uffield, W. A.,
, Mauna Ulu
otimes, v. 16,
ap of the Kau
S. Geol. Survey
le, 1:24,000.
l, G. A., 1951,
saltic rocks in
ll. 994, 98 p.
nd Peck, D. L.,
Kilauea Volcano
puhi lava lake:
73, no. 10, p.

CIETY JANUARY
PRIL 24, 1972
DIRECTOR, U.S.

GEORGE A. THOMPSON *Department of Geophysics, Stanford University, Stanford, California 94305*
DENNIS B. BURKE *Department of Geology, Stanford University, Stanford, California 94305*

Rate and Direction of Spreading in Dixie Valley, Basin and Range Province, Nevada

Note: This paper is dedicated to Aaron and Elizabeth Waters on the occasion of Dr. Waters' retirement.

ABSTRACT

The subsurface geometry of Dixie Valley indicates that for the last 15 m.y. the basin has been spreading at an average rate of at least 0.4 mm/yr. Offset Pleistocene shorelines indicate that for the last 12,000 yrs the basin has been spreading at an average rate of about 1 mm/yr. These rates are roughly consistent with geodetic measurements of historic faulting. The spreading direction obtained from large slickenside grooves on fault planes is approximately N. 55° W.—S. 55° E.

INTRODUCTION

According to plate tectonic concepts, the Pacific plate is moving northwestward relative to the North American plate. The boundary between these plates is a wide, broken zone in which one major element is the San Andreas fault system, connecting the East Pacific Rise with the Gorda Rise. Another important element in the zone is the system of faults which largely define the Basin and Range province; faulting within this province is a product of relative Pacific–North American plate movements. In contrast to the San Andreas system, however, Basin and Range faulting results from extension—or spreading—of the crust, and this faulting creates new crustal area.

We have shown (Thompson and others, 1967) that displacement on a fault segment of given strike in the Basin and Range province can be understood in terms of its components of horizontal extension and right- or left-lateral strike slip. The relation of the strike of a fault segment to the direction of spreading controls the lateral component of movement on that segment. (The vertical component is a necessary result of horizontal extension on a nonvertical fault.)

In order to understand the mechanics of the Pacific–North American plate boundary, it is important to establish both the direction and rate of spreading in the Basin and Range province. We have attempted to do this for one region which we believe to be representative of the province as a whole. Dixie Valley (Fig. 1) is one of about 20 major block-faulted basins between the Sierra Nevada to the west and the Wasatch Mountains to the east. Earthquakes and associated faulting occurred in this basin in 1903, 1915, and 1954. Three measures of fault offset for different intervals of time in Dixie Valley are available, giving three approximations of spreading rate: (1) Geodetic measurements made before and after the 1954 faulting give a measure of direction and amount of extension associated with a single earthquake. (2) Displacements of the shoreline of a late Pleistocene lake supply a measure of the extension during the last 12,000 yrs. (3) Fault displacements determined from our geophysical studies in Dixie Valley give the total amount of extension for late Cenozoic time (about 15 m.y.). The long-term direction of this extension can be determined from the average azimuth of large slickenside grooves on fault surfaces.

MEASURES OF RATE

Geodetic Measurements

The 1954 faulting showed an abrupt elastic rebound, with an extension component normal to the regional strike of the faulting, of 1.5 m (Whitten, 1957). The extent to which scarps in the alluvium of Dixie Valley have been effaced by erosion, before reactivation, suggests that displacements of this magnitude are repeated at any one place less often than every 100 yrs, but more often than every 10,000 yrs. If they occur every 1,000 yrs, the average spreading rate would be 1.5 mm/yr.

PRINTED IN U.S.A.
Geological Society of America Bulletin, v. 84, p. 627–632, 6 figs., February 1973

Pleistocene Shoreline

A late Pleistocene lake occupied Dixie Valley, isolated by surrounding mountains from the nearby basin of Lake Lahontan. Gravel beach ridges clearly record where high lake stands impinged on the alluvium of the basin. Shorelines on the bedrock of adjacent ranges are evidenced by a "bathtub ring" of calcareous tufa. The highest readily recognizable shoreline stands at about 3,585 ft above sea level but it has been tectonically tilted and faulted (Burke, 1967). The degree of preservation of the shoreline complex indicates that the highest lake stand was contemporaneous with the high stand of Lake Lahontan.

We collected two samples of calcareous tufa for carbon-14 analysis from the east front of the Stillwater Range, lat 39°54'20"N., long. 117°59'45"W., elevation approximately 3,50[illegible] ft. The ages obtained by Isotopes, Inc. are:

Sample I-3269 11,560 ± 180 yrs B.P.
Sample I-3270 11,700 ± 180 yrs B.P.

These dates are in close correspondence with tufa dates from the high shorelines in the Lahontan basin (Broecker and Kaufman, 1965) and the Searles Lake basin (G. I. Smith, 1968). Although the validity of this dating method is open to some question (Morrison, 1968), the consistency of these dates indicates that a high shoreline age of about 12,000 yrs is a reasonable assumption for present purposes.

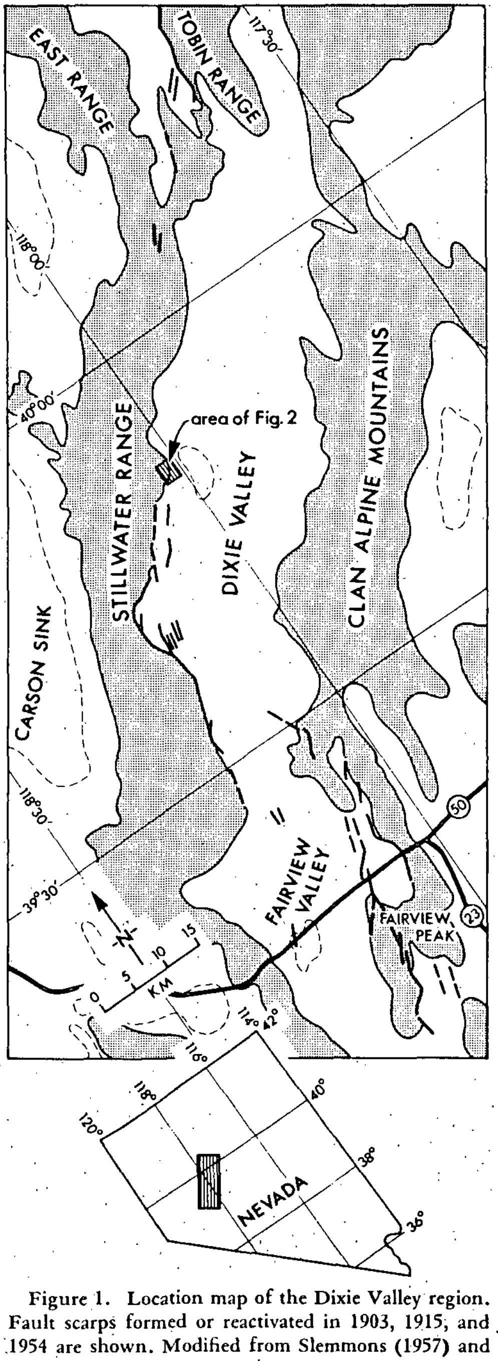

Figure 1. Location map of the Dixie Valley region. Fault scarps formed or reactivated in 1903, 1915, and 1954 are shown. Modified from Slemmons (1957) and Burke (1967).

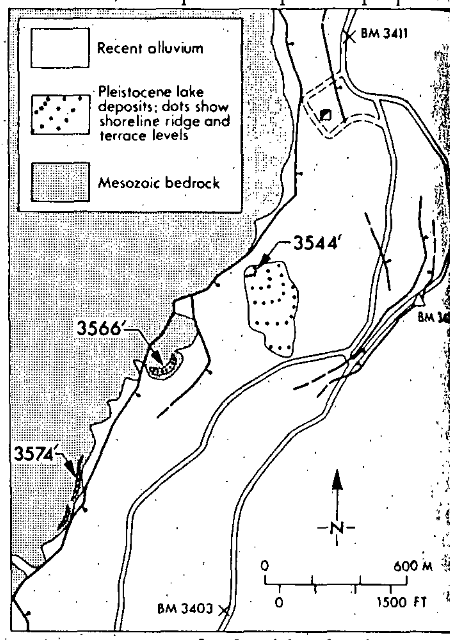

Figure 2. Map of offset lake shorelines in west-central Dixie Valley. The relative vertical spacing of beach ridges around the valley demonstrates that the highest beach ridge preserved in this area (3,544 ft) marks—like the tufa-cemented terrace deposits on bedrock—the highest lake stand.

record where high la
e alluvium of the ba
rock of adjacent ra
"bathtub ring" of
iest readily recogniz
bout 3,585 ft above
tectonically tilted
The degree of pres
complex indicates
d was contemporan
Lake Lahontan.
amples of calcareous
from the east fron
lat 39°54′20″N.,
ion approximately
by Isotopes, Inc. ar
1,560 ± 180 yrs B.P.
1,700 ± 180 yrs B.P.
ose correspondence
high shorelines in
roecker and Kaufm
Lake basin (G. I. Sm
validity of this da
ome question (Morr
of these dates indic
ge of about 12,000 yr
for present purpos

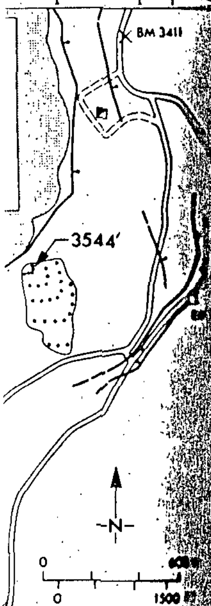

ffset lake shorelines
he relative vertical
valley demonstrates
served in this area
nented terrace deposits
tand.

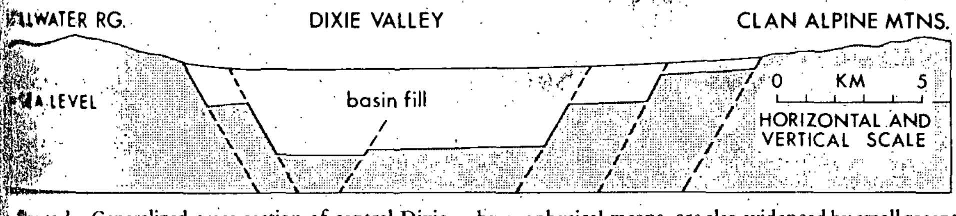

Figure 3. Generalized cross section of central Dixie Valley. Major offsets in bedrock at depth, as determined by geophysical means, are also evidenced by small recent scarps at the surface. After Burke (1967).

The shoreline deposits are offset by faults in many places; a particularly clear and measurable example is on the west side of central Dixie Valley (Fig. 2). There the vertical displacement is 9 m, and it may have occurred in two or more episodes of faulting. The fault surfaces are not exposed, and we must assume that their dip is similar to that of the many exposed faults—about 60°. Numerous scarps in the alluvium demonstrate that this offset is matched by opposing faults on the other side of the basin, and this inferred geometry is supported by seismic evidence (discussed in the next section) that shows the bedrock floor of the basin was not tilted by Basin and Range faulting. This geometry gives a vertical displacement of 9 m in the last 12,000 yrs, and a corresponding horizontal extension of 10 m in the basin during the same length of time. The average rate of extension is slightly less than 1 mm/yr.

Geophysical Exploration

A variety of geophysical techniques, including refraction seismology, gravity measurements, and magnetic depth estimates were used to determine the bedrock geometry of the valley and the subsurface dip of faults (Thompson and others, 1967; T. E. Smith, 1968). The results are summarized in Figure 3. With pre-fault topography restored, the total vertical displacement has been at least 5 km, and the horizontal extension has been 6 km or more. The time of inception of faulting is not known accurately, but Miocene-Pliocene sediments were deposited in the region in a subdued ver-

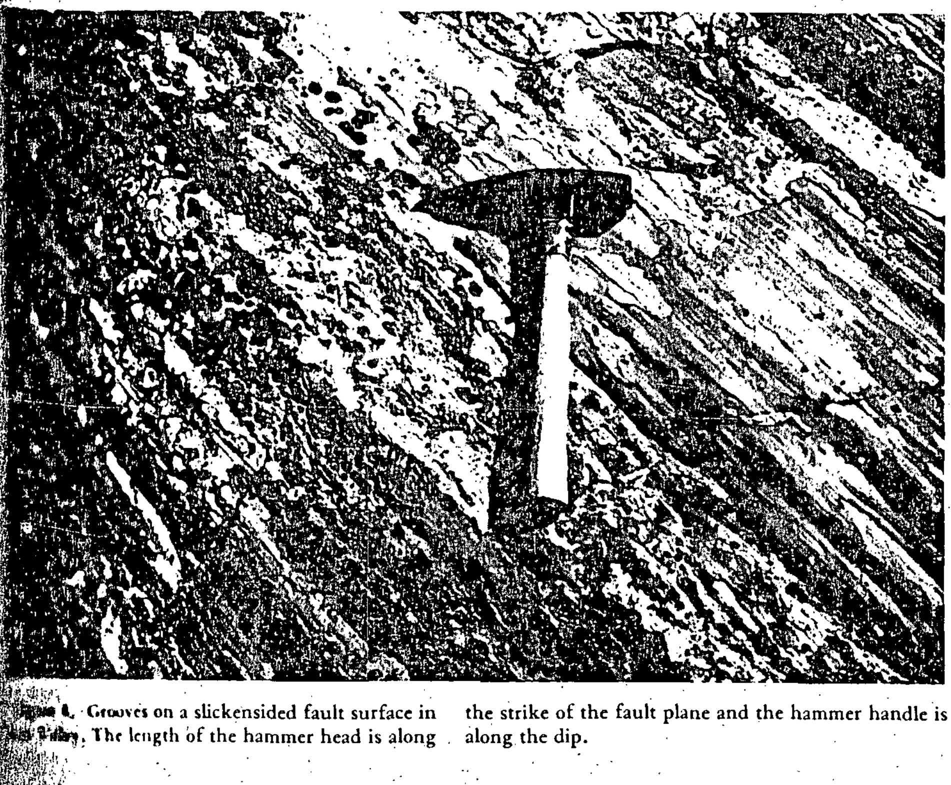

Figure 4. Grooves on a slickensided fault surface in Dixie Valley. The length of the hammer head is along the strike of the fault plane and the hammer handle is along the dip.

sion of present fault-block topography (Deffeyes, 1959), and we estimate the time to be about 15 m.y. The spreading rate, based on a minimum of 6 km of extension in 15 m.y., is at least 0.4 mm/yr.

SPREADING DIRECTION

1954 Faulting

Geodetic work, covering only the southern part of the 1954 faults, showed a general northwest-southeast extension direction on faults that have an average strike of about N. 15° E. (Whitten, 1957; Meister and others, 1968). Displacements of surface features (Slemmons, 1957) and the seismic first-motion solution (Romney, 1957) are generally consistent with the geodetic data.

Fault Grooves

Farther north in Dixie Valley itself, no consistent horizontal component of displacement was recognized in the 1954 fault breaks (Slemmons, 1957). Many older fault surfaces in bedrock are well exposed by erosion however, and grooves on these surfaces (Fig. 4) give a reliable measure of relative motion over a longer time period. A remarkable characteristic of the grooves is that their direction is generally independent of the strike of the fault segment on which they occur. The fault pattern is zigzag in plan, and when two blocks separated by a zigzag fault move apart, some fault segments would be expected to show lateral components of slip. This is exactly what is observed. For example, fault segments that strike north-south nearly always show a component of right-lateral slip. Those that strike northeast-southwest most commonly show a component of left-lateral slip.

Measurements on all grooved surfaces that could be found on the west side of Dixie Valley are compiled in Figure 5. The top histogram shows the azimuth (horizontal direction) of grooves. The mean azimuth, a little west of northwest-southeast, indicates the spreading direction. The scatter is probably caused in part by detachment and gravity sliding of small individual blocks. The bottom histogram shows the variability in fault directions (plotted as azimuth of dip direction for ease of comparison with groove direction).

The same data are shown in another way in Figure 6. The azimuth of each groove set is plotted in relation to the fault plane on which

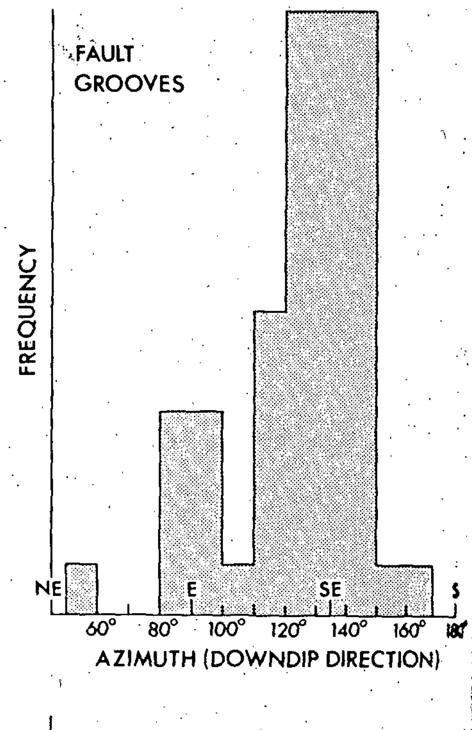

Figure 5. Histograms of the azimuths of fault plane grooves (above) and fault plane dips (below) on the western side of Dixie Valley. Fifty-four measurements for each are represented.

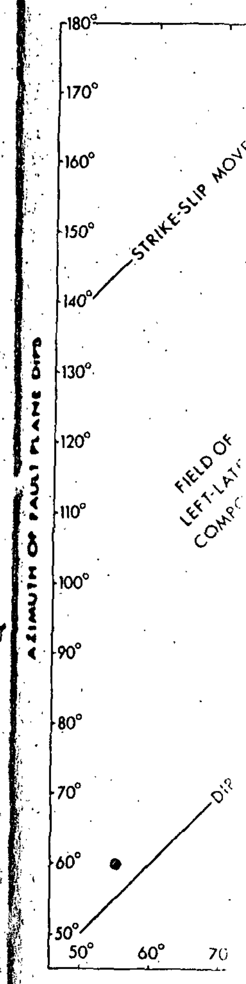

Figure 6. Plot of th... plane segments in Dixie

it occurs. To avoid a... groove set (in th... plotted against the ... fault plane dip. Th... divided between nor... and those with rig... dip. Pure dip slip is... pure strike slip were... The point "N" o... mean topographic tr... the Dixie-Fairview ... spreading direction ... is the corresponding ... and "Av" is the poin... The mean groove d...

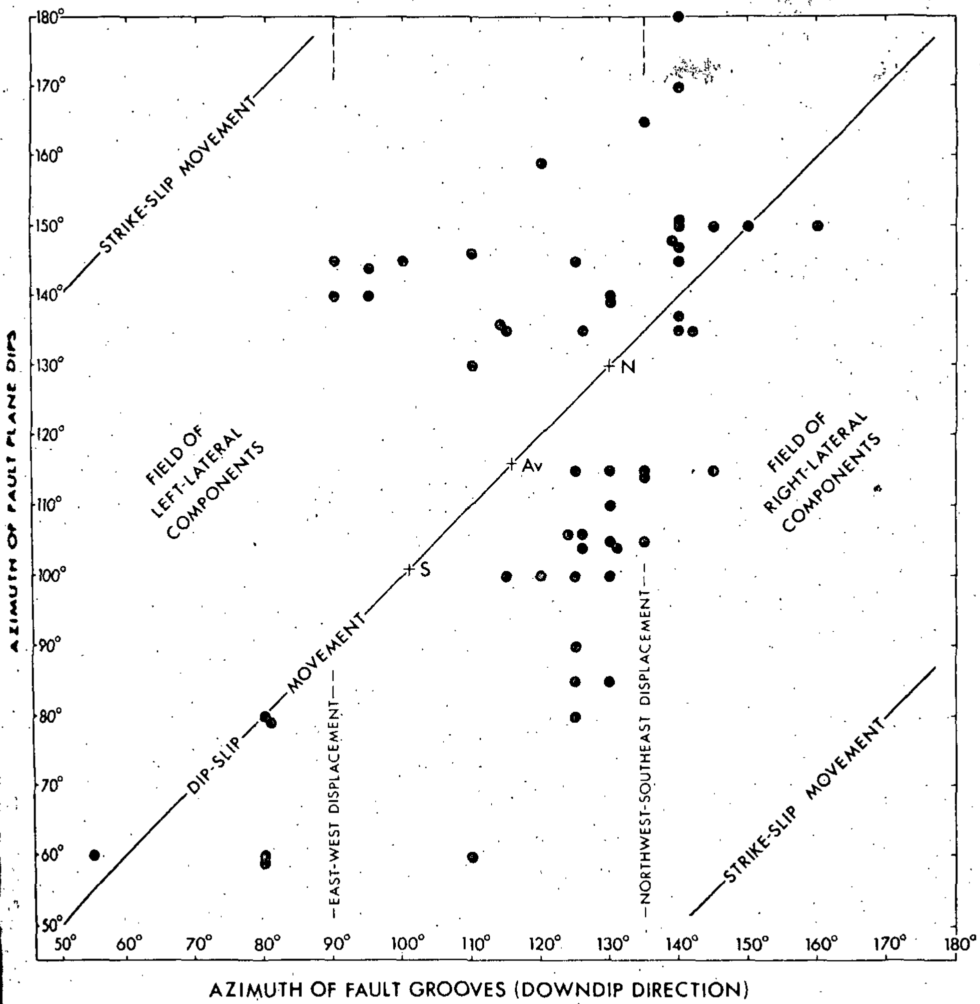

Figure 6. Plot of the azimuths of dips on fault plane segments in Dixie Valley versus the azimuth of fault grooves on those segments.

it occurs. To avoid ambiguity, the azimuth of a groove set (in the down-dip direction) is plotted against the corresponding azimuth of fault plane dip. The field is almost evenly divided between normal faults with left-lateral and those with right-lateral components of dip. Pure dip slip is rare, and no faults with pure strike slip were found.

The point "N" on Figure 6 represents the mean topographic trend of the northern half of the Dixie-Fairview basin and a hypothetical spreading direction normal to that trend. "S" is the corresponding point for the southern half, and "Av" is the point for the basin as a whole. The mean groove direction and the median groove direction both lie between 125° and 130°, to the right of "Av." This plot suggests that the basin as a whole has a slight right-lateral component of motion within it. From the average groove direction, we interpret the spreading direction to be approximately 125° or, in more conventional terms, N. 55° W.-S. 55° E. In Figure 1, this inferred spreading direction is oriented left to right on the page.

Comparative Data

We made similar groove studies in the Comstock Lode district and near Genoa, Nevada—150 to 200 km southwest of Dixie Valley. The indicated spreading direction in the Comstock district is N. 60° W.–S. 60° E.; near Genoa the direction is east-west.

Earthquakes triggered by the Benham nuclear explosion, 300 km to the southeast of Dixie Valley, released tectonic tension in a west-northwest–south-southeast direction (Hamilton and Healy, 1969). These results are surprisingly consistent with ours, and it appears that within the expected local variations—and within the uncertainties of measurement—the spreading direction is nearly constant over a wide region of the Basin and Range province.

CONCLUSIONS

For the last 15 m.y., Dixie Valley has been spreading at an average rate of at least 0.4 mm/yr; and for the last 12,000 yrs, it has been spreading at an average rate of about 1 mm/yr. The spreading direction is N. 55° W.–S. 55° E. Normal faults bounding the valley are markedly crooked, and fault segments have right- or left-lateral components of slip depending upon their strike.

The spreading direction appears to be fairly consistent over a wide region of the Basin and Range province. This direction is in harmony with the relative Pacific–North American plate motions postulated by Atwater (1970).

The 5 km of spreading in Dixie Valley, if extrapolated to the whole breadth of the Basin and Range province, suggests a total spreading of about 100 km, a 10 percent increase in crustal area.

ACKNOWLEDGMENTS

This work was supported in part by the Harry Oscar Wood Fund of the Carnegie Institution of Washington.

Basin and Range structure has been a source of geologic debate since the earliest explorations of the American West, and citation of all the literature which serves as foundation for this small report would increase our bibliography by an order of magnitude. We happily acknowledge that a paper by Fuller and Waters (1929) is an otherwise unrecorded part of our legacy. This lucid and objective report, and discussions with Aaron Waters beginning more than 25 years ago, are greatly appreciated.

REFERENCES CITED

Atwater, T., 1970, Implications of plate tectonics for the Cenozoic tectonic evolution of western North America: Geol. Soc. America Bull., v. 81, p. 3513–3536.

Broecker, W. S., and Kaufman, Aaron, 1965, Radiocarbon chronology of Lake Lahontan and Lake Bonneville II, Great Basin: Geol. Soc. America Bull., v. 76, no. 5, p. 537–566.

Burke, D. B., 1967, Aerial photograph survey of Dixie Valley, Nevada, *in* Geophysical study of basin-range structure, Dixie Valley region, Nevada: U.S. Air Force Cambridge Research Labs. Spec. Rept. 66-848.

Deffeyes, K. S., 1959, Late Cenozoic sedimentation and tectonic development of central Nevada [Ph.D. thesis]: Princeton, New Jersey, Princeton Univ., 118 p.

Fuller, R. E., and Waters, A. C., 1929, The nature and origin of the horst and graben structure of southern Oregon: Jour. Geology, v. 37, p. 204–238.

Hamilton, R. M., and Healy, J. H., 1969, Aftershocks of the Benham nuclear explosion: Seismol. Soc. America Bull., v. 59, p. 2271–2281.

Meister, L. J., Burford, R. O., Thompson, G. A., and Kovach, R. L., 1968, Surface strain changes and strain energy release in the Dixie Valley–Fairview Peak area, Nevada: Jour. Geophys. Research, v. 73, p. 5981–5994.

Morrison, R. B., 1968, Means of time-stratigraphic division and long distance correlation of Quaternary successions, *in* Morrison, R. B., and Wright, H. E., eds., Means of correlation of Quaternary successions: Internat. Cong. Assoc. Quaternary Research, 7th, Proc., v. 8, Salt Lake City, Utah Univ. Press, p. 1–113.

Romney, C., 1957, Seismic waves from the Dixie Valley–Fairview Peak earthquakes: Bull. Seismol. Soc. America, v. 47, p. 301–319.

Slemmons, D. B., 1957, Geological effects of the Dixie Valley–Fairview Peak, Nevada, earthquakes of December 16, 1954: Bull. Seismol. Soc. America, v. 47, p. 353–375.

Smith, G. I., 1968, Late Quaternary geologic and climatic history of Searles Lake, southeastern California, *in* Morrison, R. B., and Wright, H. E., eds., Means of correlating Quaternary successions: Internat. Cong. Assoc. Quaternary Research, 7th, Proc., v. 8, Salt Lake City, Utah Univ. Press, p. 293–310.

Smith, T. E., 1968, Aeromagnetic measurements in Dixie Valley, Nevada; implications on basin-range structure: Jour. Geophys. Research, v. 73, p. 1321–1331.

Thompson, G. A., Meister, L. J., Herring, A. T., Smith, T. E., Burke, D. B., Kovach, R. L., Burford, R. O., Salehi, A., and Wood, M. D., 1967, Geophysical study of basin-range structure, Dixie Valley region, Nevada: U.S. Air Force Cambridge Research Labs. Spec. Rept. 66-848.

Whitten, C. A., 1957, Geodetic measurements in the Dixie Valley area: Seismol. Soc. America Bull., v. 47, p. 321–325.

Manuscript Received by the Society April 1972